Summer 8-24-2012

Mammalian alteration/deficiency in activation 3 (Ada3) is essential for embryonic development and cell cycle progression.

Shakur Mohibi
University of Nebraska Medical Center

Channabasavaiah B. Gurumurthy
University of Nebraska Medical Center, cgurumurthy@unmc.edu

Alo Nag
Northwestern University

Jun Wang
University of Nebraska Medical Center

Sameer Mirza
University of Nebraska Medical Center, smirza@unmc.edu

THE JOURNAL OF BIOLOGICAL CHEMISTRY VOL. 287, NO. 35, pp. 29442–29456, August 24, 2012

Mammalian Alteration/Deficiency in Activation 3 (*Ada3*) Is Essential for Embryonic Development and Cell Cycle Progression*[S]

Received for publication, May 4, 2012, and in revised form, June 22, 2012 Published, JBC Papers in Press, June 26, 2012, DOI 10.1074/jbc.M112.378901

Shakur Mohibi[‡1], Channabasavaiah Basavaraju Gurumurthy[‡§1], Alo Nag[§2], Jun Wang[‡], Sameer Mirza[‡3], Yousaf Mian[§4], Meghan Quinn[‡], Bryan Katafiasz[‡], James Eudy[‡], Sanjit Pandey[‡], Chittibabu Guda[‡], Mayumi Naramura[§¶], Hamid Band[‡§‖], and Vimla Band[‡¶5]

From the [‡]Department of Genetics, Cell Biology, and Anatomy and [‖]Departments of Biochemistry and Molecular Biology, Pathology and Microbiology, and Pharmacology and Neuroscience, College of Medicine, and the [¶]Eppley Institute for Research in Cancer and Allied Diseases, University of Nebraska Medical Center, Omaha, Nebraska 68198-5805 and the [§]Department of Medicine, Evanston Northwestern Healthcare Research Institute, Northwestern University, Evanston, Illinois 60201

Background: Ada3 is a core component of HAT containing coactivator complexes.
Results: Germline deletion of *Ada3* is embryonic lethal, and cell deletion leads to abnormal cell cycle progression.
Conclusion: Ada3 is a critical protein at organismic and cellular level.
Significance: This study describes a novel role of Ada3, a component of HAT complexes, as a critical regulator of cell survival.

Ada3 protein is an essential component of histone acetyl transferase containing coactivator complexes conserved from yeast to human. We show here that germline deletion of *Ada3* in mouse is embryonic lethal, and adenovirus-Cre mediated conditional deletion of *Ada3* in $Ada3^{FL/FL}$ mouse embryonic fibroblasts leads to a severe proliferation defect which was rescued by ectopic expression of human *Ada3*. A delay in G_1 to S phase of cell cycle was also seen that was due to accumulation of Cdk inhibitor p27 which was an indirect effect of c-*myc* gene transcription control by Ada3. We further showed that this defect could be partially reverted by knocking down p27. Additionally, drastic changes in global histone acetylation and changes in global gene expression were observed in microarray analyses upon loss of Ada3. Lastly, formation of abnormal nuclei, mitotic defects and delay in G_2/M to G_1 transition was seen in *Ada3* deleted cells. Taken together, we provide evidence for a critical role of Ada3 in embryogenesis and cell cycle progression as an essential component of HAT complex.

The eukaryotic cell cycle progression depends on proper coordination of DNA replication and duplication of chromosomes to daughter cells (1), a process precisely regulated by modification of chromatin that allows the accessibility to factors involved in transcription (2). Thus, proteins involved in modulating the structure of chromatin play an important role in cell cycle progression. The post-translational modification of core histones (H2A, H2B, H3, and H4) is an essential process for altering chromatin structure (3, 4). Histone acetyl transferases (HATs)[6] and histone deacetylases are required to maintain steady state levels of acetylation (5). Several HAT enzymes, such as general control nonderepressible 5 (Gcn5), p300/CBP-associated factor (PCAF), p300, and CREB-binding protein (CBP), have been identified over the years (6, 7). Most of the HATs are part of large complexes such as the human TBP-free TAF complex (TFTC); the Spt3/Taf9/Gcn5 acetyltransferase complex (STAGA) (human homolog of yeast SAGA complex) and the Ada2a-containing (ATAC) complex that play a role in several important processes, such as cell cycle (8, 9). Additionally, previous studies from our laboratory and that of others have demonstrated the presence of p300 HAT in Ada3-containing protein complexes (10, 11). Given the combined presence of Ada3 with Gcn5 in a number of distinct HAT complexes, recent evidence for a role of Gcn5 in regulating DNA replication as well as mitosis (12–14) suggest that Ada3 may also play a role in cell cycle. Despite the range of established and potential cellular functions of Ada3 as part of multiple HAT complexes, the *in vivo* physiological role of mammalian Ada3 is not known.

We previously identified human Ada3 as a novel human papillomavirus 16 E6-binding protein (15). Human Ada3 is the

* This work was supported, in whole or in part, by National Institutes of Health Grant CA96844 and CA144027 (to V. B.) and CA87986, CA99163, CA105489, CA116552 and NCI 5U01CA151806-02 (to H. B.). This work was also supported by Department of Defense Grants W81XWH-07-1-0351 and W81XWH-11-1-0171 (to V. B.).
[S] This article contains supplemental Materials and Methods, Figs. S1–S6, and Tables S1–S3.
[1] Both authors contributed equally to this work.
[2] Present address: Dept. of Biochemistry, University of Delhi South Campus, New Delhi-110021, India.
[3] Supported by Susan G. Komen Postdoctoral Fellowship KG111248.
[4] Present address: Molecular Biology Graduate Program, Loyola University Chicago, Maywood, IL 60153.
[5] To whom correspondence should be addressed: Dept. of Genetics, Cell Biology and Anatomy, College of Medicine, 985805 Nebraska Medical Center, University of Nebraska Medical Center, Omaha, NE 68198-5805. Tel.: 402-559-8565; Fax: 402-559-7328; E-mail: vband@unmc.edu.

[6] The abbreviations used are: HAT, histone acetyltransferase; Ada3, alteration/deficiency in activation 3; hAda3, human Ada3; MEF, mouse embryonic fibroblast; Cdk, cyclin-dependent kinase; Gcn5, general control nonderepressible 5; PCAF, p300/CBP-associated factor; CBP, CREB-binding protein; CREB, cAMP-response element-binding protein; STAGA, Spt3/Taf9/Gcn5 acetyltransferase complex; ATAC, Ada2a-containing complex; adeno-Cre, adenovirus expressing the Cre recombinase; Rb, retinoblastoma protein; E, embryonic days; PI, propidium iodide; TBP, TATA-binding protein; TAF, TBP-associated factor.

homologue of the yeast Ada3, an essential component of the Ada transcriptional coactivator complex composed of Ada2, Ada3, and a HAT component Gcn5 (16). Genetic studies in yeast have demonstrated that Ada3 functions as a critical component of coactivator complexes that link transcriptional activators, bound to specific promoters, to histone acetylation and basal transcriptional machinery (17–19). We showed that Ada3 binds and stabilizes the tumor suppressor p53 protein and is required for p53 acetylation by p300 (20). Work from our laboratory has also shown that Ada3 is required for HAT recruitment to estrogen receptors and their transcription activation function (11). We and others have shown that Ada3 also associates with and regulates transcriptional activity of other nuclear hormone receptors, including retinoic acid receptor (21) and androgen receptor (22).

Here, we used conditional deletion of mouse *Ada3* gene to explore the physiological importance of mammalian Ada3. We demonstrate that homozygous deletion of *Ada3* is early embryonic lethal. *Ada3* deletion in $Ada3^{Flox/Flox}$ ($Ada3^{FL/FL}$) MEFs showed that Ada3 is required for efficient cell cycle progression through G_1 to S transition as well as for proper mitosis. Detailed analyses in this system revealed an Ada3-c-Myc-Skp2-p27 axis that controls G_1 to S phase progression and partly contributes to cell cycle delay upon *Ada3* deletion. Additionally, loss of Ada3 showed dramatic decrease in acetylation of core histones that are known to play an important role in cell cycle. Loss of Ada3 also resulted in several changes in gene expression as observed by microarray analyses. Notably, many of the genes affected were involved in mitosis. Taken together, we present evidence for an essential role of mammalian Ada3 in embryonic development and cell cycle progression.

EXPERIMENTAL PROCEDURES

Generation of Ada3 Gene-targeted Mice, Isolation of Mouse Embryos and PCR Genotyping—Details concerning generation of conditional *Ada3* knock-out construct and *Ada3* knock-out mouse as well as PCR genotyping strategies are described in the supplemental data.

Cell Culture Procedures and Viral Infections—Embryonic day 13.5 embryos were dissected from $Ada3^{FL/+}$ intercrossed females, and MEFs were isolated and immortalized following the 3T3 protocol (23). MEFs were maintained in Dulbecco's modified Eagle's medium supplemented with 10% fetal calf serum. Adenoviruses expressing EGFP-Cre or enhanced green fluorescent protein (EGFP) alone were purchased from the University of Iowa (Gene Transfer Vector Core). An adenovirus dose of 50–100 MOI diluted in 4 ml of serum-free medium was added to cells in 100-mm culture dishes (at about 30% confluence) and incubated for 1 h each at room temperature and at 37 °C followed by the addition of 7 ml of complete medium. After overnight incubation at 37 °C, medium was replaced with complete medium, and cells were carried further for various experiments. To generate retroviral FLAG-h*Ada3* vector, full-length FLAG-h*Ada3* (15) was cloned into pMSCVpuro vector (Clontech). Retroviruses were generated by transiently transfecting this retroviral construct into the Phoenix ecotropic packaging cell line using the calcium phosphate co-precipitation method. The retroviruses were transduced into $Ada3^{FL/FL}$ MEFs by three infections at 12-h intervals using supernatant from transfected Phoenix cells to generate $Ada3^{FL/FL}$ MEFs expressing FLAG-hAda3. Scrambled shRNA (5′-GGTTAAA-ACCTTACGATGT-3′) or p27 shRNA (5′-GTGGAATTTCG-ACTTTCAG-3′) was introduced into $Ada3^{FL/FL}$ MEFs by using three infections at 12-h intervals of the shRNA bearing pSUPER.retro.puro (Oligoengine) retrovirus containing supernatants from Phoenix cells. Retroviral infections were carried out in the presence of 8 μg/ml Polybrene (Sigma) and were followed by selection in 2 μg/ml puromycin for 48 h until complete loss of uninfected cells.

Proliferation Assay, Colony Formation Efficiency Assay, and Cell Cycle Analysis—To perform proliferation assays, 1 day after adenovirus infection, cells were plated at different numbers in 6-well plates in triplicates (5×10^4 (for counting on day 3), 2.5×10^4 (for counting on day 5), 1.25×10^4 (for counting on day 7), and 0.625×10^4 (for counting on day 9) and counted at the indicated time points. For colony formation assay, cells 3 days after adenovirus-infection were trypsinized and plated at 1000 cells per 100-mm culture dishes in triplicates and carried for 15 more days with medium change as required. At the end of incubation, colonies in dishes were fixed and stained with crystal violet solution (0.25% crystal violet in 25% methanol) and photographed. For cell cycle analysis, 2 days after plating and adenoviral infection of 2×10^5 cells in 100-mm culture dishes, cells were synchronized by replacing the complete medium with DMEM + 0.1% FCS and incubating for 72 h. Synchronized cells were stimulated with complete medium (DMEM + 10% FCS) for various time points and harvested and stained with propidium iodide (PI) for FACS analysis. For synchronization of cells at G_2/M phase, 48 h after adenovirus infection, cells were switched to complete medium containing 125 ng/ml nocodazole for 18 h. Following synchronization, cells were washed three times with PBS and stimulated with complete medium for various time points and analyzed by FACS after PI staining.

Generation of Ada3 Monoclonal Antibody and Immunoblotting—Antibodies used in this study can be found in the supplemental data.

In Vitro Kinase Assay—*In vitro* kinase assay was performed using purified histone H1 (Roche Applied Science) or Rb (769) (Santa Cruz Biotechnology sc-4112) as a substrate. Adenovirus-infected MEFs were starved for 3 days and stimulated with serum. Cells were harvested in lysis buffer (20 mM Tris-HCl (pH 7.5), 150 mM NaCl, 0.5% Nonidet P-40, 0.1 mM Na_4VO_3, 1 mM NaF, and protease inhibitor mixture), and cyclin-dependent kinase (Cdk) complex was recovered by immunoprecipitation with 2 μg of either anti-Cdk4 (sc-56277)/Cdk6 (sc-53638) antibodies mixture or anti-Cdk2 (sc-6248) antibody (Santa Cruz Biotechnology). Cdk4/6 or Cdk2 complexes were captured with protein G-agarose for 1 h and washed with lysis buffer followed by one wash with kinase buffer (50 mM Tris-HCl (pH 7.5), 7.5 mM $MgCl_2$, 1 mM dithiothreitol, 0.1 mM Na_4VO_3, and 1 mM NaF). Cdk2 complex was incubated with histone H1 (2 μg) or Rb (500 ng), whereas Cdk4/6 complex was incubated with only Rb (500 ng) in kinase buffer containing 10 mM β-glycerophosphate, 33 μM ATP, and 10 μCi of [γ-^{32}P]ATP (10 mCi/ml, 6000 Ci/mmol) at room temperature for 20 min. The products were

subjected to SDS-PAGE, transferred to polyvinylidene difluoride membranes (PVDF), and autoradiographed.

Analysis of the p27 Protein Turnover—*Ada3*$^{FL/FL}$ MEFs were plated in 100-mm dishes and infected with control or Cre adenoviruses. For analyzing p27 protein half-life in exponentially growing cells, 2 days after adenovirus infection, cells were treated with 50 μg/ml cycloheximide (Sigma) and harvested at the indicated time points. For analyzing p27 protein half-life in serum-starved cells, 2 days after adenovirus infection, cells were starved for 72 h in 0.1% serum-containing medium. Subsequently, 50 μg/ml cycloheximide was added to the medium, and cells were harvested at the indicated time points. Total cell extracts were prepared, and equivalent amounts were run on SDS-PAGE and analyzed by Western blotting. Densitometry analysis was carried out on scanned images using ImageJ software.

RNA Extraction and Quantitative Real-time PCR—TRIzol reagent (Invitrogen) was used to isolate total RNA from MEFs infected with control virus or Cre adenovirus. 2 μg of total RNA was used for reverse transcriptase reaction using SuperScript™ II reverse transcriptase (Invitrogen). Real-time PCR quantification was performed in triplicates using SYBR Green PCR master mix (Applied Biosystems) and the primers listed in supplemental Table S3. Expression levels were normalized against β-actin mRNA levels, and the results were calculated by the $\Delta\Delta C_t$ method.

Chromatin Immunoprecipitation Experiments—Approximately 0.7 million *Ada3*$^{FL/FL}$ MEFs were plated in 100-mm dishes and infected with control or Cre adenoviruses. Forty-eight hours after infection, cells were synchronized with DMEM + 0.1% FCS for 72 h and then stimulated with complete medium (DMEM + 10% FCS) for 0–60 min as indicated for each experiment in Fig. 8*C*. ChIP experiment was performed by using the ChIP-IT Express kit from Active Motif. PCR amplification was performed using primers for the c-*myc* enhancer (forward, 5′-CTAGAACCAATGCACAGAGC-3′; reverse, 5′-CTCCCAGGACAAACCCAAGC-3′) and for the *Skp2* promoter (forward, 5′-GCCATCGAGACCCCGGAGAT-3′; reverse, 5′-TGAGTCCCTTCCAGACGCTGT-3′). Control PCR was performed using primers for the c-*myc* distal site (forward, 5′-ACACACCTTGAATCCCGT-3′; reverse, 5′-CCCAGCTAGAATGAAGAAG-3′) and the *Skp2* distal site (forward, 5′-GTGCTAGCTGCTTACCTTTGT-3′; reverse, 5′-GATAAGGATGCACTCTGGGGC-3′). PCR products were analyzed on 2% agarose/Tris-acetate-EDTA gels with ethidium bromide stain. PCR of the input DNA prior to immunoprecipitation was used as a control.

Generation of Recombinant Baculoviruses and Ada3-His Expression Using Bac-to-Bac® Expression System—Ada3 baculoviral construct information and recombinant protein purification are detailed in the supplemental data.

HAT Assay—Protocol used for *in vitro* HAT assay can be found in the supplemental data.

Microarray Analyses—Protocol for microarray analyses is described in the supplemental data. The microarray data from this publication have been submitted to the GEO database and have been assigned the following Series record: GSE37542.

TABLE 1
Genotype analysis of embryos from heterozygous intercrosses

Stage	Total no. of embryos	No. (%) of embryos			
		WT	Heterozygous	KO	Resorbed
Live born	224	75 (33)	149 (66)	0	0
E12.5	14	3 (21)	5 (36)	0	6 (43)
E 9.5	15	8 (53)	2 (13)	0	5 (33)
E 8.5	44	12 (27)	27 (61)	0	5 (11)
E 3.5	15	4 (27)	7 (47)	4 (27)	0

RESULTS

Deletion of Ada3 Leads to Early Embryonic Lethality in Mice—The targeting construct generated using the recombineering technique (supplemental Fig. S1*A*; see supplemental Materials and Methods) was electroporated into an ES cell line derived from the 129/Ola strain of mice. Screening of resultant neomycin-resistant colonies yielded three correctly targeted clones (supplemental Fig. S1*B*). One positive clone was microinjected into blastocysts. The resulting chimeras transmitted the targeted allele to their progeny as verified by PCR. The neomycin cassette flanked by Frt recombination sites was removed by crossing the *Ada3*-targeted mice to FlpE recombinase transgenic mice (B6.Cg-Tg (ACTFLPe) 9205Dym/J; stock number 005703). Homozygous *Ada3*$^{FL/FL}$ mice were viable and fertile and exhibited no gross abnormalities when compared with *Ada3*$^{FL/+}$ or *Ada3*$^{+/+}$ controls. To achieve *Ada3* deletion, heterozygous *Ada3*-targeted mice (*Ada3*$^{FL/+}$ mice) were bred with transgenic mice expressing the adenovirus EIIa promoter-driven Cre (B6.FVB-Tg (EIIa-Cre) C5379Lmgd/J). EIIa directs Cre expression in a wide range of tissues including germ cells. Heterozygous *Ada3*-targeted, Cre transgene-positive mice were crossed to C57BL/6J (wild-type) mice to generate heterozygous *Ada3*-deleted, Cre transgene-negative (*Ada3*$^{+/-}$) mice. Heterozygous *Ada3*$^{+/-}$ mice of a mixed 129/Sv × C57BL/6 background were viable and fertile, and their median life span of more than 18 months was comparable with that of their control littermates (data not shown). Heterozygous *Ada3*$^{+/-}$ mice were intercrossed to obtain homozygous *Ada3*-null mice. No *Ada3*$^{-/-}$ mice were observed among 224 live born pups screened (Table 1). The ratio of wild type to heterozygous offspring was 1:2, indicating that the loss of one *Ada3* allele does not lead to haploinsufficiency in mice.

To assess the specific period of developmental failure in the *Ada3* knock-out mice, embryos derived from *Ada3*$^{+/-}$ intercrosses were genotyped at different stages of gestation using a duplex PCR method (supplemental Fig. S1, *C* and *D*). Because no homozygous mutant embryos were recovered beyond embryonic day 8.5 (E8.5; Table 1), blastocysts were isolated at 3.5 days postcoitum and genotyped directly by PCR (supplemental Fig. S1*E*). When compared with blastocysts of *Ada3*$^{+/+}$ and *Ada3*$^{+/-}$ genotypes, *Ada3*$^{-/-}$ blastocysts that attached to culture dishes showed severe growth retardation of the trophoblast layer, and the inner cell mass was absent (supplemental Fig. S1*F*). PCR analysis revealed that ~25% of blastocysts analyzed were null for *Ada3* (Table 1). These results demonstrate that Ada3 plays a critical role in early embryogenesis in mice. The failure of *Ada3*$^{-/-}$ embryos to remain viable beyond E3.5 suggests a potential role of Ada3 in cell proliferation because

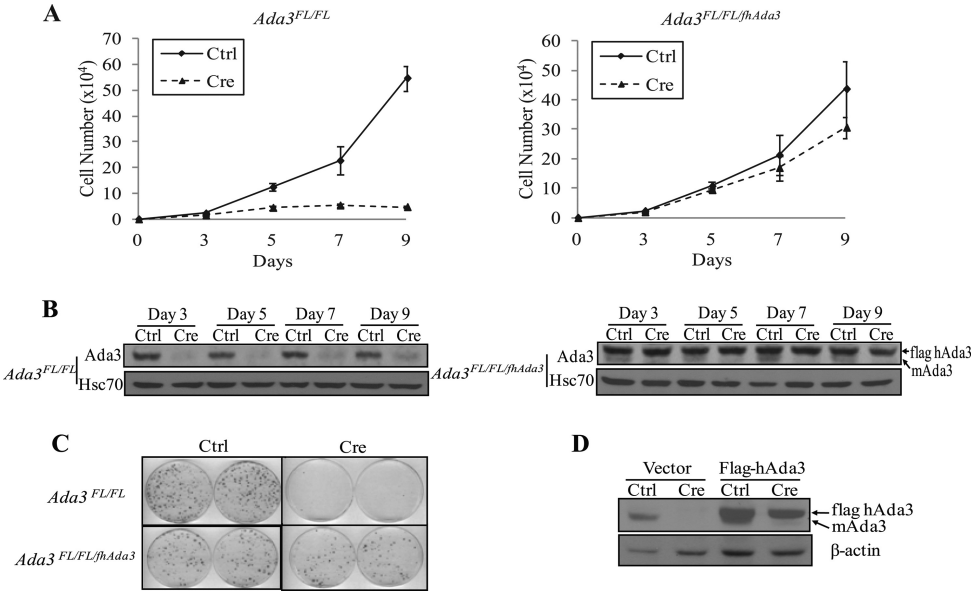

FIGURE 1. **Ablation of Ada3 causes proliferation defect in MEFs.** *A*, growth curves of *Ada3*$^{FL/FL}$ (*left*) and *Ada3*$^{FL/FL/fhAda3}$ (*right*) MEFs after control adenovirus (*Ctrl*)or Cre adenovirus (*Cre*) infection. Data are mean ± S.E. from three independent experiments performed in triplicates. *B*, Ada3 protein levels at different time points after Cre adenovirus infection. Note that reconstituted control cells express both mouse (*mAda3*; *lower band*) and human (FLAG hAda3; *upper band*) proteins, whereas only hAda3 is seen in Cre adenovirus-infected cells. *C*, colony formation assay. Crystal violet staining of the indicated cells infected with control virus or Cre adenovirus grown for 10 days is shown. *D*, Western blotting of lysates from *C* showing exogenous and endogenous Ada3.

extensive cellular proliferation occurs during this early stage of embryogenesis (see later sections).

Ada3 Is Ubiquitously Expressed in Adult Mouse Tissues—Embryonic lethality of *Ada3*$^{-/-}$ mice suggested a potential role of Ada3 in growth and development of many tissues. To examine whether Ada3 is expressed in adult tissues, we analyzed the relative levels of Ada3 protein expression in a range of adult mouse tissues. For this purpose, lysates from various tissues of 8-week-old wild-type mice were subjected to immunoblotting using an anti-Ada3 monoclonal antibody generated in our laboratory (see supplemental Materials and Methods). As seen in supplemental Fig. S2, Ada3 is ubiquitously expressed in all the tissues with higher levels seen in the mammary gland, lung, and thymus. These results suggest potentially ubiquitous functional roles of Ada3 and are consistent with embryonic lethal phenotype of its germline deletion.

Conditional Ada3 Deletion in MEFs Leads to Proliferation Arrest—Given the embryonic lethality as a result of *Ada3* deletion, we resorted to a cellular model of conditional *Ada3* deletion to investigate its roles at the cellular level. For this purpose, we generated *Ada3*$^{FL/FL}$ mice by interbreeding *Ada3*$^{FL/+}$ mice and established MEFs from these mice. Conditional *Ada3* deletion was obtained by infecting *Ada3*$^{FL/FL}$ MEFs with an adenovirus expressing the Cre recombinase (adeno-Cre), with adeno-GFP serving as a control. To assess the effects of Ada3 on cell proliferation, equal numbers of control- and adeno-Cre-infected MEFs were plated a day after adenoviral infection, and cells were counted at the indicated time points up to 9 days. Notably, *Ada3*-deleted MEFs exhibited a significantly slower rate of proliferation when compared with control MEFs (Fig. 1*A*, *left*). To confirm that the defect in cell proliferation was specifically due to depletion of Ada3, we generated *Ada3*$^{FL/FL/hAda3}$ MEFs by retrovirally introducing human *Ada3* (h*Ada3*) with an N-terminal FLAG tag into *Ada3*$^{FL/FL}$ MEFs. These transfectants were verified to be expressing the exogenous FLAG-tagged Ada3 protein (Fig. 1*B*). Similar to *Ada3*$^{FL/FL}$ MEFs, adeno-Cre infection of these cells led to deletion of endogenous *Ada3* and loss of its protein product (Fig. 1*B*). Notably, however, Cre-mediated deletion of *Ada3* in *Ada3*$^{FL/FL/hAda3}$ MEFs had a minimal effect on the proliferation of MEFs, whereas similar treatment of *Ada3*$^{FL/FL}$ MEFs led to reduction in the rate of proliferation; thus, the proliferative defect induced by deletion of mouse *Ada3* in MEFs was rescued by exogenous hAda3 (Fig. 1*A*, *right*). Colony formation efficiency assay, as an independent method to measure the extent of cell proliferation, further confirmed the proliferative defect of *Ada3*-deleted MEFs that could be rescued by reconstitution with exogenous hAda3 (Fig. 1, *C* and *D*).

Ada3 Is Required for Cell Cycle Progression through G_1 to S Phase—We reasoned that the proliferation defect upon *Ada3* deletion in MEFs could reflect a role of Ada3 in cell cycle progression. To directly examine whether Ada3 plays a role in cell cycle progression, *Ada3*$^{FL/FL}$ MEFs were infected with control and Cre adenoviruses, arrested in G_0/G_1 by serum deprivation for 72 h, and then synchronously released into cell cycle by serum stimulation. FACS-based cell cycle analysis of propidium iodide-stained cells showed significant delay in G_1 to S progression in *Ada3*-deleted MEFs when compared with control MEFs (Fig. 2*A*). Of note, the relative distribution of S phase in *Ada3*-null MEFs after 20 h of serum stimulation was about half (31.6 ± 2.33 S.E. %) of the control virus-infected MEFs (56.05 ± 4.71 S.E. %) (Fig. 2*B*). These results demonstrate that conditional deletion of *Ada3* leads to delay in G_1 to S progression in MEFs, indicating an essential role of Ada3 in efficient G_1/S progression.

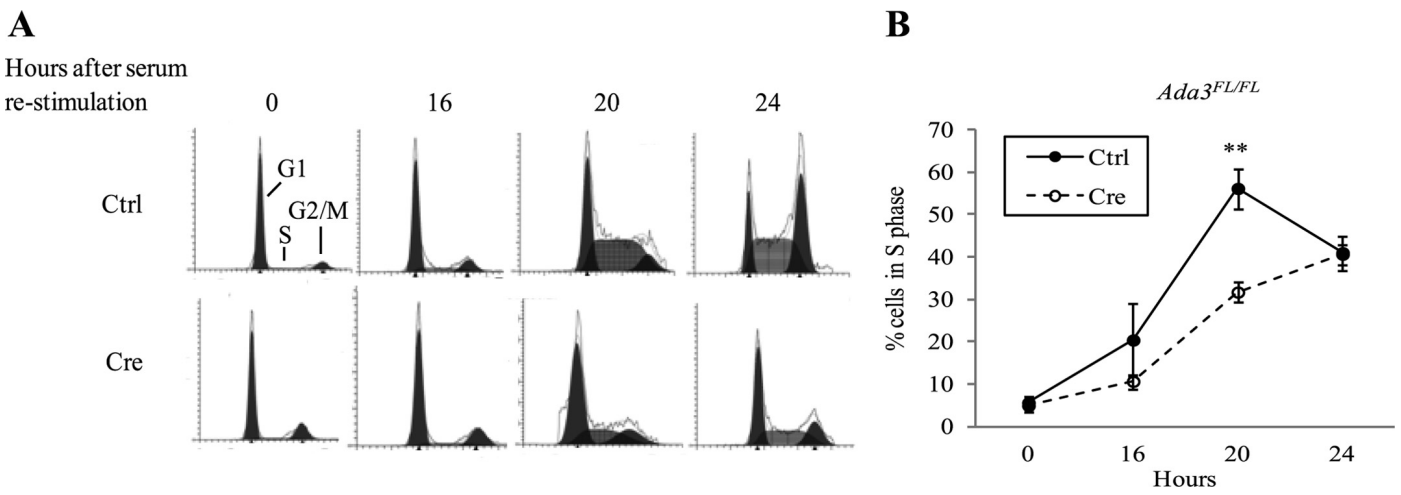

FIGURE 2. ***Ada3* disruption delays G_1 to S transition in MEFs.** *A*, control (*Ctrl*)- or Cre- infected $Ada3^{FL/FL}$ MEFs were serum-starved for 72 h and then released from synchrony as described under "Experimental Procedures" and processed for PI staining followed by FACS analysis. Cells in different phases of the cell cycle are shown from a representative experiment. *B*, graph derived from three independent experiments performed as in *A*, showing the proportion of cells entering into S phase at the indicated times after serum restimulation. *Error bars* are mean ± S.E. from three independent experiments (**, $p = 0.0096$, two-tailed Student's *t* test).

Elevated $p27^{Kip1}$ Levels and Impaired Rb Phosphorylation upon Conditional Ada3 Deletion—Given the delay in G_1/S progression imposed by induced Ada3 deficiency, we examined the status of key proteins known to control the G_1/S transition. A well established and critical event during G_1 to S progression is the phosphorylation of Rb by Cdk complexes (particularly complexes containing Cyclins D, E, or A), such as Cdk4/6 and Cdk2 (24, 25); phosphorylation of Rb leads to its release from Rb/E2F complexes, relieves E2Fs from repression, and facilitates the expression of E2F-responsive genes important for S phase progression (24, 25). Furthermore, degradation of Cdk inhibitors, such as p27, is required for progression of cells from G_1 to S phase (26, 27). Therefore, we carried out Western blotting of cell lysates obtained from control *versus* conditional *Ada3*-deleted MEFs released into synchronous cell cycle progression to assess the levels of proteins relevant to the G_1 to S phase transition. Notably, although minimal to no changes were observed in the levels of Cdk2, Cdk4, Cdk6, p16, p21, cyclin E, and cyclin D, a significant increase in p27 levels, a delay in the cell cycle-associated increase in cyclin A levels, and a lower level of Rb phosphorylation were observed in MEFs upon *Ada3* deletion when compared with control cells (Fig. 3*A*).

In view of increased levels of p27 without a significant change in the levels of Cdk proteins in cells with *Ada3* deletion, we assessed the level of Cdk2 kinase activity using an i*n vitro* kinase assay on immunoprecipitates from cells. Although the Cdk4/6 kinase activity was comparable between control- and adeno-Cre-infected MEFs (Fig. 3*B*), the level of Cdk2 kinase activity was substantially reduced in Cre-infected MEFs when compared with control MEFs (Fig. 3*B*). These results suggest the potential reduction of Cdk2 kinase activity in the *Ada3*-deleted cells as a result of an increase in the levels of p27, accounting for defective Rb phosphorylation.

Accumulation of p27 upon Ada3 Deletion Is due to Increased Stability of p27—As accumulation of p27 levels upon *Ada3* deletion appeared to be functionally important, we examined whether this accumulation was at the transcriptional or post-transcriptional level. Real-time PCR analysis showed that serum stimulation resulted in a marked reduction in the levels of *Cdkn1b* mRNA in both the control-infected and the Cre-infected cells (Fig. 4*A*); furthermore, the levels of *Cdkn1b* mRNA at various time points after serum addition remained comparable between the two cell populations, reinforcing the idea that the increase in p27 protein levels in *Ada3*-deleted cells was likely to be at a post-transcriptional level. As alterations in protein stability are a prominent mechanism to control Cdk inhibitor levels (28), we compared the half-life of p27 protein in WT *versus Ada3*-deleted MEFs using two distinct experimental formats; the first one utilized exponentially growing cultures, whereas the second one utilized cells first arrested in G_1 by serum deprivation for 72 h followed by synchronous release into cell cycle by serum addition. In each case, $Ada3^{FL/FL}$ MEFs infected with control or Cre adenoviruses were treated with cycloheximide to block new protein synthesis, and p27 levels in cell lysates following cycloheximide treatment were quantified using immunoblotting at various time points. Previous work has shown that p27 half-life in exponentially growing MEFs is about 3 h and increases to about 8 h in serum-starved cells (29). We found the p27 half-life in cells infected with control adenovirus was consistent with published results, *i.e.* approximately 2 h and 40 min in exponentially growing MEFs, whereas in growth-arrested cells, half-life was approximately 3 h and 30 min (Fig. 4, *B–E*). Notably, in both experimental formats, we observed a substantial increase in p27 protein half-life upon Cre-dependent *Ada3* deletion, with approximate half-lives of 4 h and 10 min and 6 h in exponentially growing *versus* synchronous culture formats, respectively. These results strongly support our conclusion that accumulation of p27 protein upon *Ada3* deletion is due to its increased stability.

Depletion of p27 from Conditionally Deleted Ada3 MEFs Causes a Partial Rescue of G_1/S Progression Defects—Reduced activity of the p27 target Cdk2 in *Ada3*-deleted MEFs strongly suggested a role for p27 in defective cell cycle progression in these cells. To directly establish whether this is the case, we generated stable p27 knockdown $Ada3^{FL/FL}$ MEFs ($Ada3^{FL/FL/p27shRNA}$) by infecting $Ada3^{FL/FL}$ MEFs with a retro-

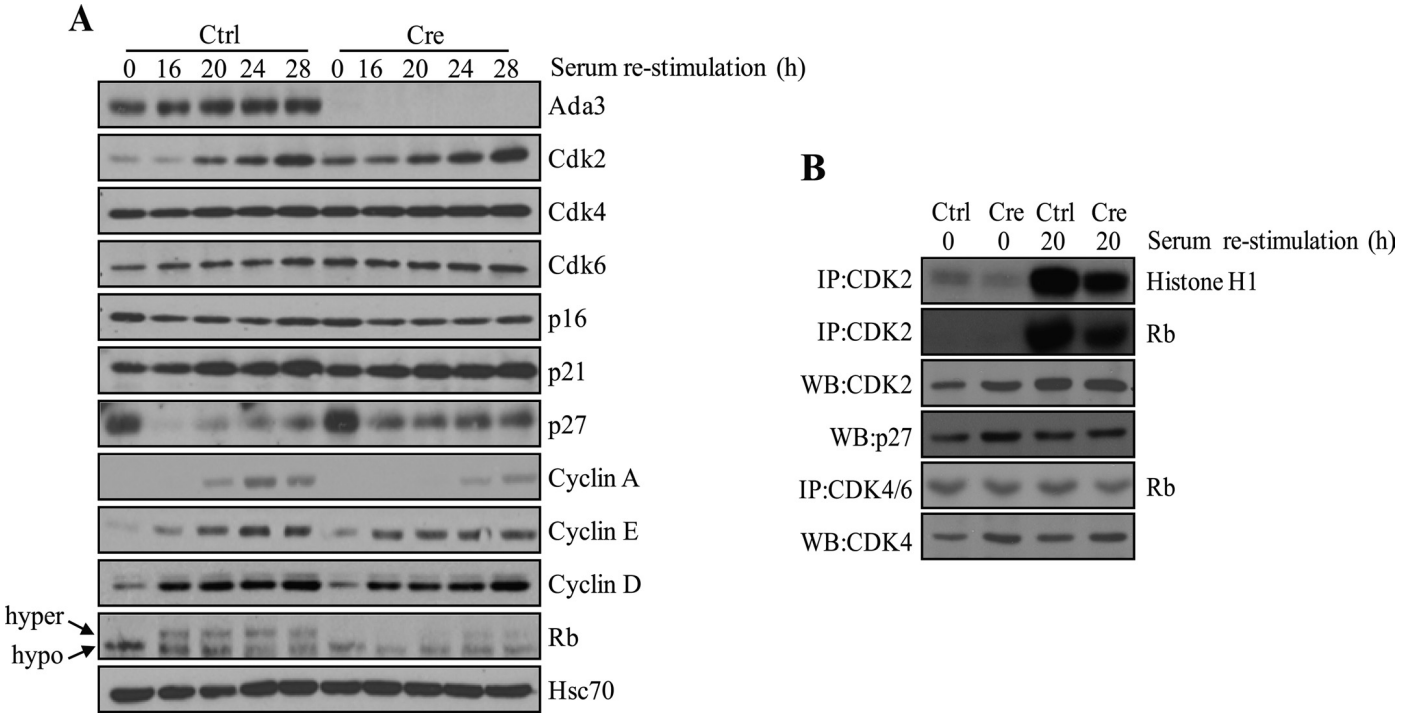

FIGURE 3. **Effect of Ada3 depletion on expression of cell cycle regulator proteins and Cdk2 kinase activity.** *A*, *Ada3*$^{FL/FL}$ MEFs infected with control (*Ctrl*) and Cre adenoviruses serum-starved for 72 h, released from synchrony as described under "Experimental Procedures," and processed for immunoblot analysis of the indicated cell cycle proteins. *hyper*, hyperphosphorylated; *hypo*, hypophosphorylated. *B*, anti-Cdk2 or anti-Cdk4/6 immunoprecipitations performed using 300-μg extracts of *Ada3*$^{FL/FL}$ MEFs infected with control or Cre adenovirus were subjected to *in vitro* kinase assay using histone H1 or Rb as a substrate. *WB*, Western blot; *IP*, immunoprecipitation.

virus expressing a p27-specific shRNA followed by selection in puromycin, which resulted in a significant knockdown of p27 expression in these cells (Fig. 5*A*). Next, we infected the *Ada3*$^{FL/FL/p27shRNA}$ MEFs with control or Cre adenovirus and analyzed these for cell cycle progression using serum deprivation followed by serum stimulation, as above (Fig. 5*B*). Notably, a partial but clear rescue of the G_1/S delay was observed in p27 shRNA-expressing cells, as seen by a much larger percentage of cells entering the S phase (41.4 ± 3.5 S.E. % in p27shRNA expressing conditionally deleted *Ada3* MEFs *versus* 31.6 ± 2.33 S.E. % in Ada3-deleted MEFs at 20 h; compare Fig. 5*C* with Fig. 2*B*). Importantly, the levels of cyclin A, which is known to be expressed during G_1/S transition and to peak in the S phase, as well as hyperphosphorylation of Rb, were essentially fully rescued by p27 shRNA knockdown (Fig. 5*D*; compare with Fig. 3*A*). Taken together, these results clearly demonstrate an important role of Ada3-dependent control of p27 levels in promoting cell cycle progression.

Deletion of Ada3 Leads to Reduced Protein and mRNA Levels of Skp2 and c-Myc—Given the causal link established above between p27 accumulation and G_1/S cell cycle delay upon *Ada3* deletion, we wished to examine the molecular mechanism by which loss of Ada3 promotes p27 stability. Published studies have established a major role of Skp2-containing E3 ubiquitin ligases in regulating p27 protein turnover during cell cycle progression (30). As *Skp2* is a transcriptional target of c-Myc (31) and Ada3-containing STAGA complex has been shown to increase *myc* mRNA transcription (32, 33), the possibility of an Ada3-c-Myc-Skp2-p27 regulatory pathway appeared to be a plausible mechanism for our findings. To explore this hypothesis, we first examined the effects of *Ada3* deletion on the levels of Skp2 mRNA (real-time PCR) and protein (immunoblotting). For this purpose, *Ada3*$^{FL/FL}$ cells infected with control or Cre adenovirus were serum-deprived and released into synchronous cell cycle progression by adding serum followed by analyses of Skp2 mRNA and protein at various time points. Notably, Skp2 mRNA and protein levels were substantially lower at each comparable time point in adeno-Cre-infected *versus* control MEFs (Fig. 6, *A* and *B*). These results indicate that *Ada3* deletion indeed leads to reduction in Skp2 levels and that this effect is likely due to reduced *Skp2* gene transcription.

Next, we asked whether *Ada3* deletion alters c-Myc mRNA levels and whether Ada3 directly binds to c-*myc* promoter. Indeed, analysis of control *versus* *Ada3*-deleted MEFs stimulated with serum to undergo cell cycle progression demonstrated that c-Myc mRNA as well as protein levels were significantly lower at each time point examined upon deletion of *Ada3* from cells (Fig. 6, *C* and *D*). Consistent with this, we observed lower occupancy of mouse *Skp2* promoter by c-Myc upon deletion of *Ada3*, which supports our results (supplemental Fig. S3). Finally, to establish that Ada3 indeed participates in the enhancement of *myc* gene transcription, we carried out ChIP analysis to assess whether Ada3 is recruited to c-*myc* enhancer during cell cycle progression. Indeed, a rapid recruitment of Ada3, as well as RNA polymerase II (used as positive control), to c-*myc* enhancer at −1.4 kb relative to transcription start site (but not to a distal site at −5 kb) was seen upon serum stimulation of MEFs (Fig. 6*E*). As expected, we did not detect any signals after immunoprecipitation with anti-Ada3 antibody in cells infected with adeno-Cre. These results therefore sup-

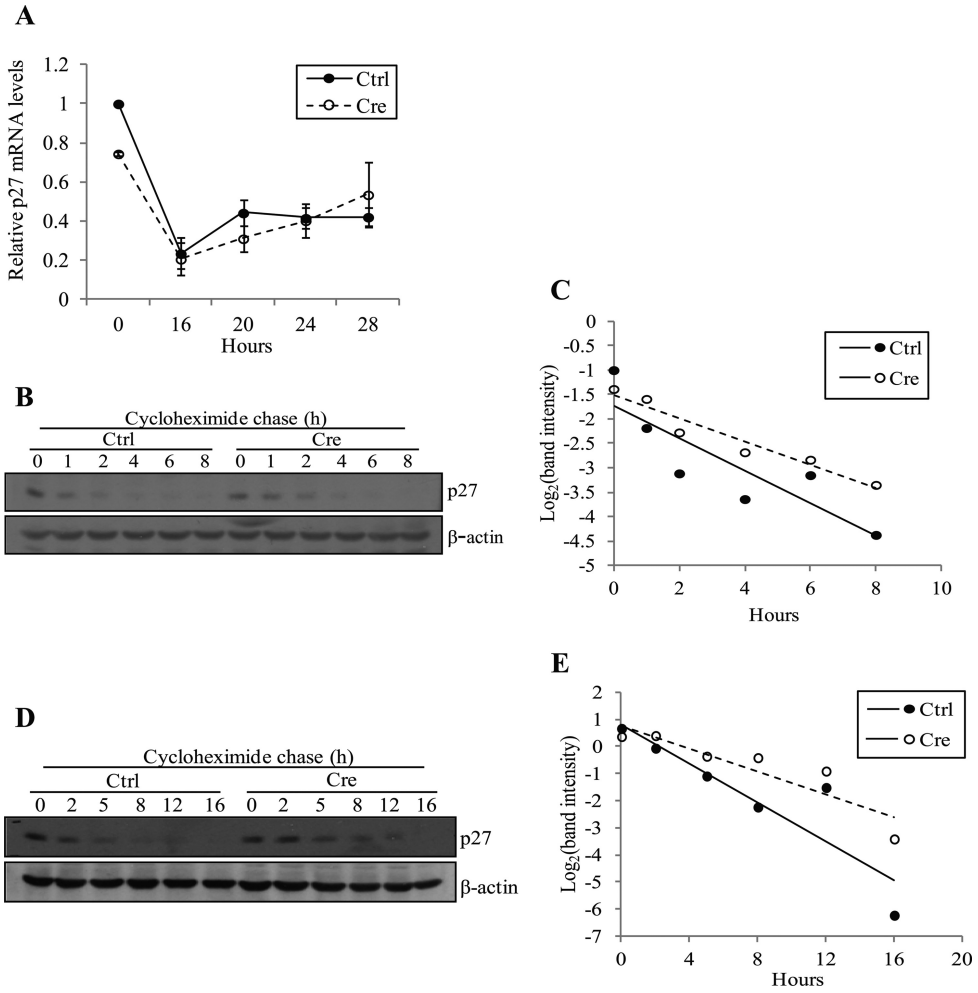

FIGURE 4. **Deletion of *Ada3* does not affect p27 transcription but extends p27 protein half-life.** *A*, unaltered p27 mRNA levels after *Ada3* deletion. Real-time RT-PCR analysis of p27 mRNA levels from cells as treated in Fig. 2 was performed. Signals were normalized to β-actin levels and plotted relative to the level of p27 mRNA in starved control (*Ctrl*) cells. *Error bars* show mean ± S.E. from three independent experiments. *B–E*, *Ada3* deletion in MEFs extends p27 half-life. *B*, 48 h after adenovirus infection, MEFs were treated with 50 μg/ml cycloheximide and harvested at the indicated time points, and p27 and β-actin protein levels were analyzed by immunoblotting. *C*, the intensity of p27 bands was quantified by densitometry, normalized to β-actin using ImageJ software, and plotted against the time of cycloheximide treatment. Each decrease of 1 unit of log 2 is equivalent to one half-life. The lines were generated by linear regression formula. *D*, after 48 h of adenovirus infection, MEFs were starved using 0.1% serum-containing medium for 72 h and subsequently treated with 50 μg/ml cycloheximide and harvested at the indicated time points. Cell lysates were analyzed by Western blotting using antibodies against p27 and β-actin. *E*, graph made from experiment in *D* by using the same procedure as in *C*.

port the existence of a novel cell cycle-associated, Ada3-regulated signaling pathway that promotes G_1/S cell cycle progression by regulating p27 stability through Myc-dependent control of *Skp2* expression.

Ada3 Deletion Leads to Decreased Histone Acetylation—As we observed a partial rescue of G_1/S transition in *Ada3*-deleted MEFs after knockdown of p27, we speculated that Ada3 deletion-induced cell cycle arrest may involve other pathways as well. Given the known literature on Ada3 as part of HAT complexes (8, 9), we examined whether Ada3 is involved in controlling global histone acetylation. Therefore, we assessed the effect of *Ada3* deletion on lysine acetylation of various core histones. We expressed Cre recombinase in $Ada3^{FL/FL}$ MEFs and harvested protein samples from asynchronous cultures after 3 days of infection. Western blotting using antibodies against important acetylated lysine residues of all four core histones (H2A-K5, H2B-K5, H3-K9, H3-K56, and H4-K8) showed a significant reduction in acetylation at all these sites in *Ada3*-deficient MEFs when compared with control MEFs (Fig. 7*A*), indicating that Ada3 is essential in maintaining global histone acetylation.

We further examined the effect of *Ada3* deletion on acetylation of core histones after synchronizing cells in G_1 phase and subsequent release. There was a dramatic down-regulation of H3-K9 acetylation and a slight decrease in acetylation of H2B-K5 in *Ada3*-deleted MEFs when compared with control-MEFs, whereas this defect was rescued in $Ada3^{FL/FL}$ MEFs reconstituted with exogenous human FLAG-Ada3 (Fig. 7*B*), suggesting that the defect in histone acetylation seen in *Ada3*-deleted MEFs was a consequence of *Ada3* deletion. Histone acetylation has been shown to be important for deposition of histones during replication-coupled nucleosome assembly as well as for chromatin maturation following DNA replication (34, 35). Thus, the partial rescue in G_1 to S transition observed upon knockdown of p27 in *Ada3*-deficient cells could be attributed to massive histone acetylation defects, which would create difficulties for cells to undergo DNA replication and thus delay transition through S phase.

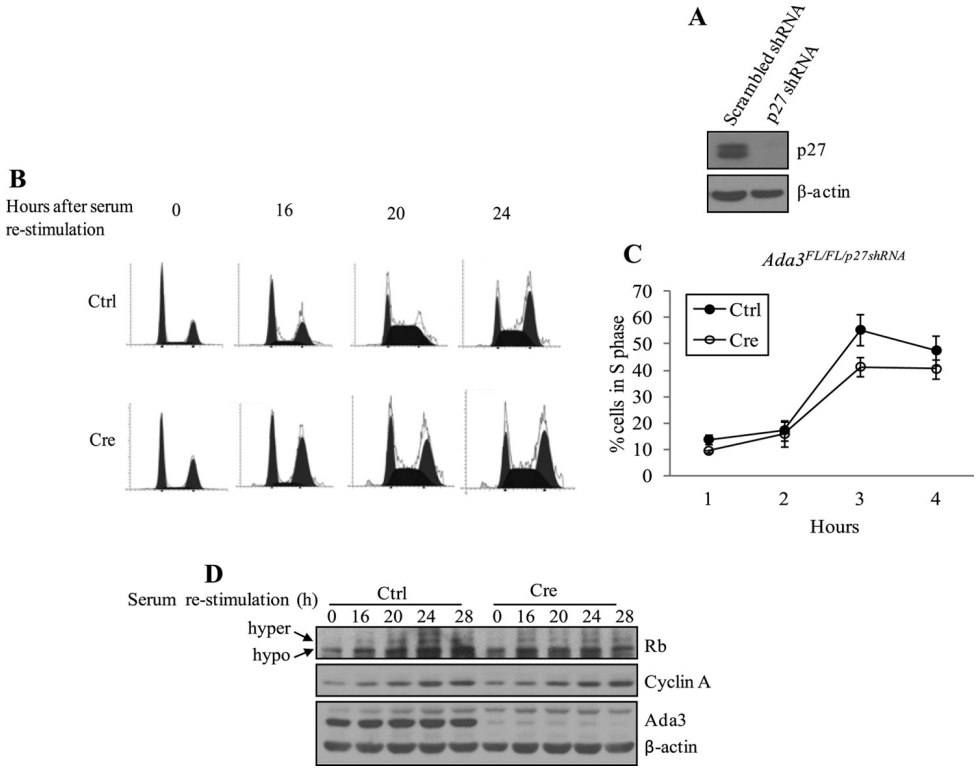

FIGURE 5. **p27 depletion partially rescues G_1 to S transition defects seen in *Ada3*-null MEFs.** *A*, *Ada3*$^{FL/FL}$ MEFs were infected with retrovirus-expressing scrambled or p27 shRNA followed by selection for 2 days in puromycin and analyzed by immunoblotting using p27 and β-actin antibodies. *B*, PI staining and FACS analysis of *Ada3*$^{FL/FL}$ MEFs expressing p27 shRNA that were infected with either control (*Ctrl*) or Cre adenoviruses and synchronized as in Fig. 2. *C*, graph derived from three experiments as in *B* showing the proportion of cells entering into S phase at the indicated times after serum restimulation. *Error bars* indicate mean ± S.E. from three independent experiments. *D*, immunoblotting of protein samples from *B* showing rescue of hyperphosphorylated (*hyper*) Rb and cyclin A levels. *hypo*, hypophosphorylated.

Recombinant Ada3 Stabilizes HAT Enzymes and Enhances Their Activity—Ada3 protein has been identified as an important component of protein complexes containing HAT enzymes. Therefore, we subjected samples harvested after 3 days of *Ada3* deletion to immunoblotting with two important HATs such as p300 and PCAF. Indeed, deletion of *Ada3* caused drastic down-regulation of p300 and PCAF in MEFs (Fig. 7*C*). Notably, *Ada3* deletion had no effect on the mRNA levels of p300 and PCAF (data not shown). Thus, the defects in histone acetylation seen in *Ada3*-null MEFs could be attributed to the effect of *Ada3* deletion on stability of important HATs in cells.

In addition to the role of Ada3 in stability of HAT enzymes, we explored whether Ada3 catalyzes the activity of HAT enzymes. Although Ada3 is shown to be important in maintaining stability of HAT complexes, it has not been demonstrated whether Ada3 directly modulates the activity of known HAT enzymes such as p300. Thus, we expressed and purified baculoviral hAda3 and used it in an *in vitro* assay in which HAT activity of p300 histone acetyl transferase enzyme on histone substrates was measured. As seen in Fig. 7*D*, increasing amounts of Ada3 resulted in increased acetylation of histone H1 and histone H3 by p300, suggesting that Ada3 plays an important role in enhancing the HAT activity of p300. To further explore the role of Ada3 in histone acetylation, we used only histone H3 as a substrate and observed an Ada3 dose-dependent increase in acetylation of histone H3 by p300 (Fig. 7*E*). Thus, Ada3 manifests its effect on histone acetylation by maintaining the integrity of various HAT complexes and by enhancing the catalytic activity of HATs.

Deletion of Ada3 Leads to Global Gene Expression Changes—Given the links between Ada3 and transcriptional activation, we used control and *Ada3*-deleted cells to perform microarray analyses. As expected, the expression of multiple genes was altered; 539 genes were down-regulated and 928 genes were up-regulated ≥ 1.5-fold upon Ada3 deletion (supplemental Table S1). Validation of some of the deregulated genes from microarray by real-time PCR showed good co-relation with the microarray data (supplemental Fig. S4). Ingenuity pathway analyses showed that most of the genes affected were involved in controlling cell growth, proliferation, and cell death (supplemental Table S2, top biological functions affected; cell growth and proliferation (386 genes) and cell death (359 genes)). The top network affected was the RNA post-transcriptional modification and cellular assembly and organization network, whereas the cell cycle, endocrine system development and function, and cancer network was the third most affected network (supplemental Fig. S5). Notably, *c-myc* and *Skp2* genes that we described above were down-regulated 1.4- and 1.43-fold, respectively. This is lower than what we observed by real-time PCR and could be attributed to the fact that microarray data were performed on asynchronous populations, whereas the real-time PCR data were performed on synchronous cells (Fig. 6, *A* and *C*). Interestingly, many of the genes present in cell growth and proliferation set were those involved in controlling cell division as well as some involved in DNA replication (Table 2).

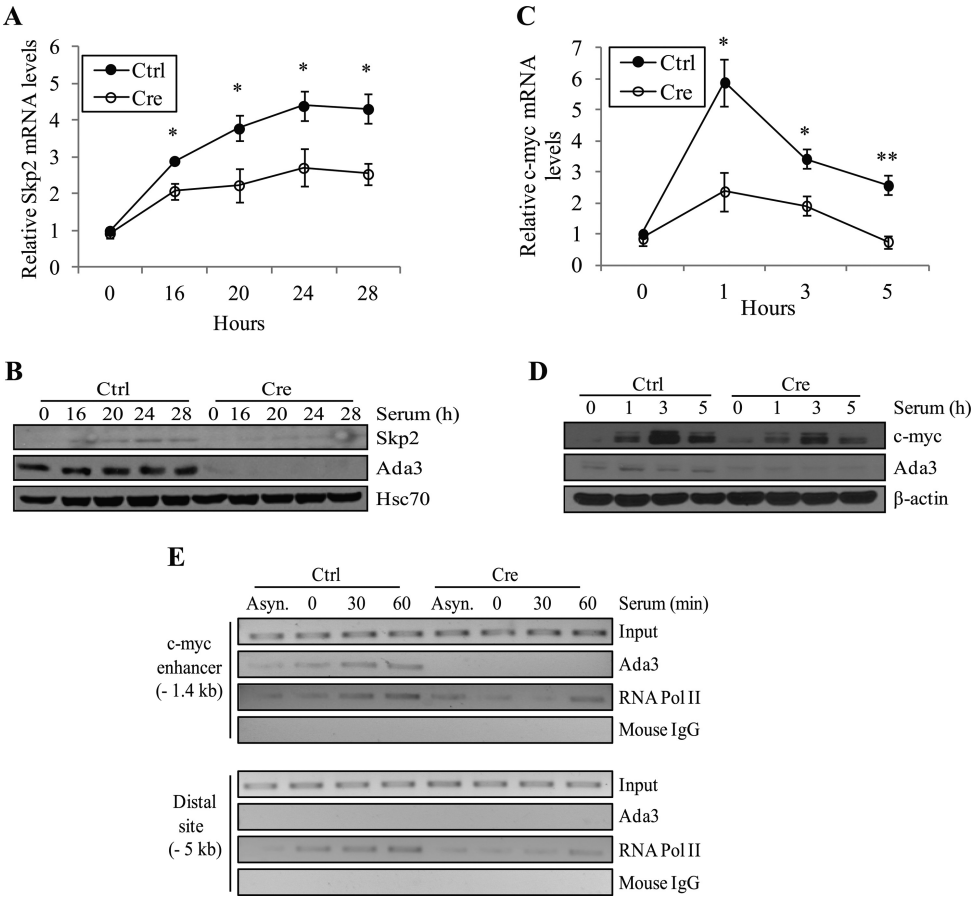

FIGURE 6. **Deletion of *Ada3* from MEFs leads to reduced mRNA and protein levels of Skp2 and c-Myc.** *A*, analysis of Skp2 mRNA levels by real-time RT-PCR from cells as treated in Fig. 2. Signals were normalized to β-actin levels and plotted relative to the level of Skp2 mRNA in starved control cells. *Error bars* represent mean ± S.E. from three independent experiments (*, $p = 0.015$, 0.036, 0.043, and 0.032 for 16, 20, 24, and 28 h, respectively by two-tailed Student's *t* test). *B*, immunoblots showing Skp2 protein levels in cells treated as in *A*. *C*, analysis of c-Myc mRNA levels by real-time RT-PCR from cells as treated in Fig. 5. Signals were normalized to β-actin levels and plotted as in *A*. *Error bars* show mean ± S.E. from three independent experiments. *D*, immunoblots showing c-Myc protein levels in cells treated as in *C* (*, $p = 0.023$ and 0.027 for 1 and 3 h, respectively; **, $p = 0.008$ by two-tailed Student's *t* test). *E*, occupancy of Ada3 on the c-*myc* enhancer. Chromatin fragments from control (*Ctrl*) and Cre *Ada3*$^{FL/FL}$ MEFs cells were immunoprecipitated with anti-Ada3 antibody. Chromatin fragments were prepared from Asynchronous (*Asyn.*) cells as well as from cells synchronized with 0.1% serum containing DMEM for 72 h (*lane 0*) and stimulated with serum with indicated time points. The immunoprecipitated DNA was analyzed by PCR, using c-Myc enhancer-specific primers. Primers amplifying a region that is 5 kb upstream of the c-Myc enhancer were used as a negative control. *RNA Pol II*, RNA polymerase II.

Ada3 Deletion Leads to Defects in Cell Division and Accumulation of Abnormal Nuclei—Based on our microarray analyses where several mitotic genes were affected upon deletion of *Ada3* and a recent study showing the role of Ada3 in mitosis upon shRNA deletion (14), we examined the effect of Ada3 deletion on mitotic phase of cell cycle. These analyses showed that Cre-mediated *Ada3* deletion led to increased accumulation of cells with abnormal nuclei when compared with control MEFs. *Ada3*-deficient MEFs showed various nuclear abnormalities such as fragmentation, lobulation, and multinucleation (Fig. 8*A*). When compared with 13.08 ± 2.39 S.E. % control MEFs, 83.41 ± 3.45 S.E. % of *Ada3*-deficient MEFs showed abnormal nuclei (Fig. 8*B*). Live imaging of cells for 24 h showed that the majority of *Ada3*-deleted cells failed to divide normally. Some of the cells snapped back while attempting to undergo cytokinesis, leading to the formation of binucleated cells, whereas other cells that had normal nucleus before mitosis showed fragmented nuclei afterward and were unable to divide. In other cases, cell division resulted in the formation of anucleated daughter cells (Representative images shown in supplemental Fig. S6). Taken together, these results demonstrate an indispensable role of Ada3 in normal cell cycle progression. The cell division defect results reported here corroborate with an earlier published study showing similar defects upon shRNA knockdown of Ada3 (14). Mitotic defects observed in their study were attributed to acetylation of a non-histone substrate cyclin A, and no changes in histone acetylation upon knockdown of Ada3 were reported. In contrast, we observed a dramatic change in global histone acetylation and expression of various genes involved in mitosis. Although at present we cannot explain this discrepancy, the differences in the results may be partly attributable to the use of different cellular systems and differences in approaches followed such as shRNA or Cre-mediated to delete *Ada3*.

Deletion of Ada3 Leads to Delay in G_2/M to G_1 Progression—As deletion of *Ada3* in MEFs led to defects in cell division, we reasoned that the disruption of Ada3 should exert an effect on G_2/M to G_1 transition. To examine this effect, we synchronized control- and Cre-adenovirus-infected *Ada3*$^{FL/FL}$ MEFs at

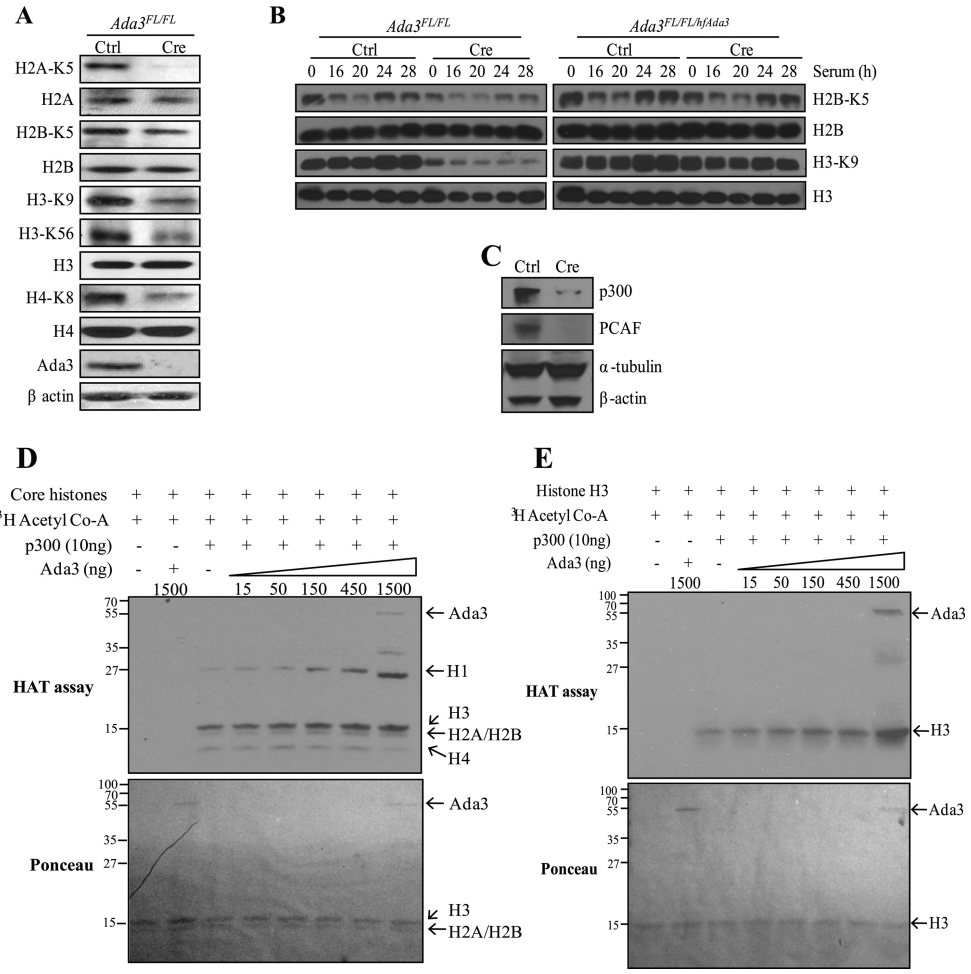

FIGURE 7. ***Ada3* deletion abrogates histone acetylation by destabilizing various HATs.** *A–C*, Western blotting analysis of lysates from asynchronous (*A* and *C*) or serum-restimulated (*B*) *Ada3*$^{FL/FL}$ or *Ada3*$^{FL/FL/fhAda3}$ MEFs infected with control (*Ctrl*) or Cre adenoviruses using the indicated antibodies. *D* and *E*, Ada3 enhances p300 HAT activity. *In vitro* HAT assay using purified recombinant human Ada3 and core histones (*D*) or histone H3 alone (*E*) along with their respective Ponceau blots to indicate equal loading is shown.

G_2/M checkpoint by treating them with nocodazole and released them from synchrony followed by cell cycle analysis using flow cytometry (Fig. 8*C*). Nocodazole-synchronized *Ada3*-deleted MEFs showed a lower percentage of cells in G_2/M phase (61%) at the 0-h time point when compared with control MEFs (80%) (Fig. 5*C*). On the contrary, we observed a higher percentage (20%) of *Ada3*-deleted MEFs in G_1 phase when compared with control MEFs (7%) after synchronization. We speculate that *Ada3*-deficient MEFs that are exhibiting a delay in G_1 to S transition were unable to get completely synchronized at G_2/M checkpoint as these cells are potentially moving slowly through the G_1 to S transition and require a prolonged treatment with nocodazole to show a complete synchronization as seen in control MEFs. When we compared the percentage of cells moving into G_1 phase on release from nocodazole treatment in both *Ada3*-deficient and control MEFs, a significant impairment in G_2/M to G_1 transition in *Ada3*-deleted MEFs was observed (Fig. 8*D*). Taken together, these results demonstrate a critical role of Ada3 in both G_1 to S transition as well as G_2/M to G_1 transition in MEFs, indicating that the cell proliferation defect observed in *Ada3*-deficient MEFs is due to a combined defect in G_1 to S as well as G_2/M to G_1 transition.

DISCUSSION

Regulated cell cycle entry and progression are essential for precise developmental programs as well as to maintain organ homeostasis in adult animals. Although the basic components of cell cycle have been largely defined, regulatory control mechanisms that ensure orderly proliferative responses to physiological cues and whose aberrations underlie the vast instances of altered proliferation in cancer continue to be elucidated. We previously identified the ADA complex component Ada3 as a human papillomavirus E6 oncoprotein partner as well as a coactivator of cell cycle checkpoint regulator and tumor suppressor p53 (15, 20). Several *in vitro* studies have shown that Ada3 is an essentially universal component of a multitude of HAT-based transcriptional regulatory complexes (8, 9), and it has become essential to define its physiological roles using *in vivo* animal models.

Here, we demonstrate that Ada3 is essential for embryonic development in mice and that *Ada3*-null embryos undergo very early lethality. As an essential component of the transcriptional coactivator complexes that include HATs and promote histone acetylation of key gene targets, Ada3 is known to be essential for growth in yeast (16) as well as in model metazoan organisms

TABLE 2

List of deregulated genes involved in cell division and DNA replication

Genes down-regulated at least 1.5-fold upon loss of Ada3 as obtained from microarray analyses. The genes were classified based upon gene ontology biological processes.

Gene symbol	Gene title	-Fold down-regulated
Genes involved in cell division		
Kifc1	Kinesin family member C1, similar to Kifc1 protein	2.0
Nfkbil1	Nuclear factor of [kappa[light polypeptide gene enhancer in B-cells inhibitor-like 1	2.0
Fbxo5	F-box protein 5	1.8
Cenpf	Centromere protein F	1.8
Cdc6	Cell division cycle 6 homolog (*Saccharomyces cerevisiae*)	1.7
Kntc1	Kinetochore-associated 1	1.7
Baz1b	Bromodomain adjacent to zinc finger domain, 1B	1.6
Mlf1ip	Myeloid leukemia factor 1 interacting protein	1.6
Myh10	Myosin, heavy polypeptide 10, non-muscle	1.6
Kif11	Kinesin family member 11	1.6
Ccna2	Cyclin A2	1.6
Smc2	Structural maintenance of chromosomes 2	1.6
Plk1	Polo-like kinase 1 (*Drosophila*)	1.5
Bub1b	Budding uninhibited by benzimidazoles 1 homolog, β (*S. cerevisiae*)	1.5
Aspm	asp (abnormal spindle)-like, microcephaly-associated (*Drosophila*)	1.5
Anln	Anillin, actin-binding protein	1.5
Zwilch	Zwilch, kinetochore-associated, homolog (*Drosophila*)	1.5
Mki67	Antigen identified by monoclonal antibody Ki 67	1.5
Mad2l1	MAD2 mitotic arrest deficient-like 1 (yeast)	1.5
Smc4	Structural maintenance of chromosomes 4	1.5
Cdca8	Cell division cycle-associated 8	1.5
Kif20b	Kinesin family member 20B	1.5
Hells	Helicase, lymphoid-specific	1.5
Ccnb1	Cyclin B1	1.5
Cdca3	Cell division cycle-associated 3	1.5
Nuf2	NUF2, NDC80 kinetochore complex component, homolog (*S. cerevisiae*)	1.5
Ndc80	NDC80 homolog, kinetochore complex component (*S. cerevisiae*)	1.5
Birc5	Baculoviral IAP repeat-containing 5	1.5
Bub1	Budding uninhibited by benzimidazoles 1 homolog (*S. cerevisiae*)	1.5
Suv39h2	Suppressor of variegation 3–9 homolog 2 (*Drosophila*)	1.5
Aurkb	Aurora kinase B	1.5
Wee1	WEE 1 homolog 1 (*Schizosaccharomyces pombe*)	1.5
Genes involved in DNA replication		
Kitl	Kit ligand	1.9
Prim1	DNA primase, p49 subunit	1.7
Mcm7	Minichromosome maintenance-deficient 7 (*S. cerevisiae*)	1.7
Ccne2	Cyclin E2	1.7
Pola1	Polymerase (DNA directed), alpha 1	1.7
Dtl	Denticleless homolog (*Drosophila*)	1.7
Cdc6	Cell division cycle 6 homolog (*S. cerevisiae*)	1.7
Chtf18	CTF18, chromosome transmission fidelity factor 18 homolog (*S. cerevisiae*)	1.7
Nfib	nuclear factor I/B	1.6
Prim1	DNA primase, p49 subunit	1.6
Orc1l	Origin recognition complex, subunit 1-like (*S. cerevisiae*)	1.6
Rrm1	Ribonucleotide reductase M1	1.6
Rpa1	Replication protein A1	1.6
Cdt1	Chromatin licensing and DNA replication factor 1	1.6
Gins2	GINS complex subunit 2 (Psf2 homolog)	1.5
Rbbp4	Retinoblastoma-binding protein 4	1.5
Chaf1b	Chromatin assembly factor 1, subunit B (p60)	1.5
Tk1	Thymidine kinase 1	1.5

such as *Drosophila* where Ada3 deficiency is associated with arrest in early development (36). However, this study is the first direct demonstration of an essential role of Ada3 in mammalian embryonic development. Notably, the embryonic developmental block imposed by *Ada3* deletion occurs very early, resulting in arrest of development at the blastocyst stage, the stage of embryonic development at which extensive cell proliferation occurs (37). Notably, studies that employed gene knockouts of subunits of several chromatin-modifying complexes, including *Gcn5*, *Trrap*, *Ep300*, *CBP*, *Hdac3*, or *Atac2*, also lead to early embryonic lethality (34, 38–42), consistent with an essential role of chromatin modification machinery in mammalian growth and development. However, except for *Trrap* knockout, which produces lethality at the blastocyst stage (42), knockouts of other genes produce embryonic developmental arrest at much later stages: for example, *Gcn5* (E9.5–E11.5), *Ep300* (E9.5–E10.5), and *Atac2* (E11.5) in comparison with E3.5 block observed in *Ada3*-null mice. The relatively early developmental arrest of *Ada3*-null mice when compared with other regulators could reflect the role of Ada3 as a component of multiple chromatin-remodeling complexes (see Introduction and below). The distinct times of arrest seen with *Gcn5*-null and *Ada3*-null embryos are somewhat surprising and suggest the possibility that Ada3 may mediate early developmental roles through complexes in which Gcn5 is not a critical component or is functionally redundant with other HATs. Consistent with this hypothesis, we observed that *Ada3*-deleted cells exhibit defects in multiple histone acetylations and show decrease in the levels of PCAF and p300 proteins.

We used the conditional deletion feature of the mouse model to assess the critical functional roles of Ada3 by utilizing Cre-dependent gene deletion in MEFs from $Ada3^{FL/FL}$ mice. This system provided a clear evidence that Ada3 plays an essential

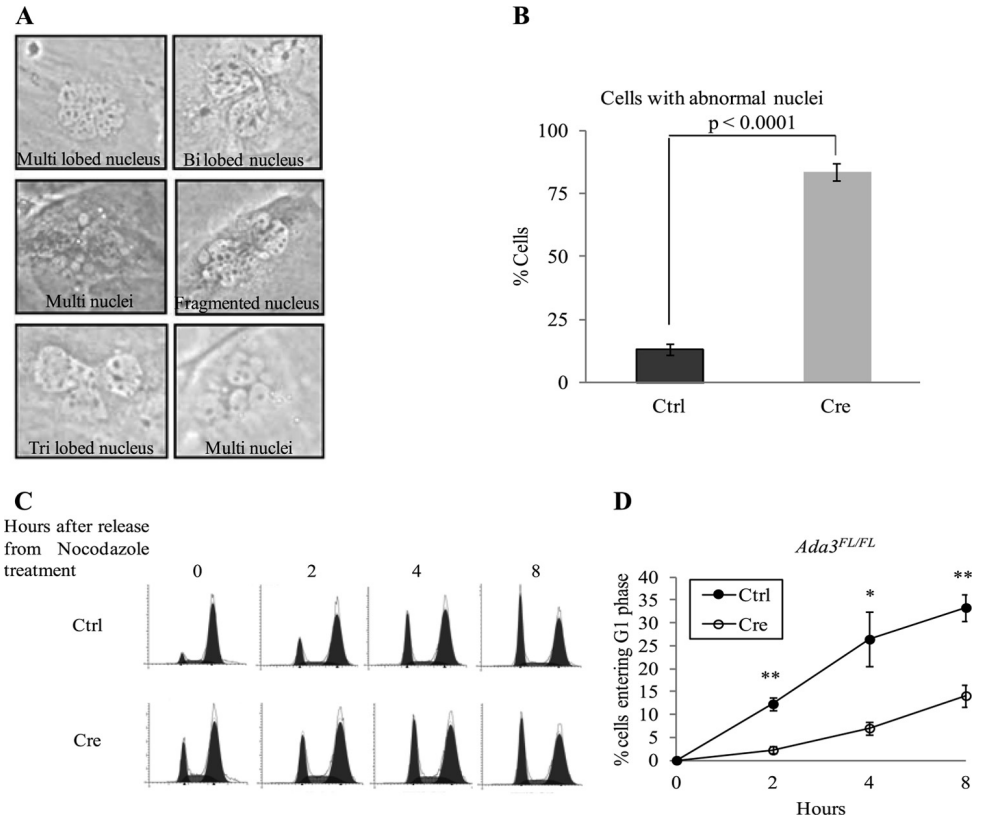

FIGURE 8. **Abnormal cell division and delayed G_2/M to G_1 transition in *Ada3*-deleted cells.** *A*, images of *Ada3*$^{FL/FL}$ cells after 5 days of infection with Cre adenovirus showing abnormal (fragmented, lobulated, or multi) nuclei. *B*, quantification of abnormal nuclei from cells infected with control (*Ctrl*) or Cre adenovirus; 5 days after infection, cells were fixed and stained with Giemsa stain and scored for abnormal nuclei (at least 100 cells from each group were counted). *Error bars* show mean ± S.E. from three independent experiments. *C*, control- and Cre adenovirus-infected MEFs were treated for 20 h with nocodazole and were harvested at the indicated time points after release, stained with PI, and subjected to FACS analysis. *D*, graph showing the percentage of cells entering G_1 phase after release from nocodazole treatment at various time points from experiments as in *C*. *Error bars* are mean ± S.E. from three independent experiments (*, $p = 0.034$; **, $p = 0.0038$ and 0.007 for 4 and 8 h, respectively, by two tailed Student's *t* test).

role in cell proliferation by promoting G_1 to S as well as G_2/M to G_1 cell cycle progression. Furthermore, the proliferative arrest imposed by conditional deletion of *Ada3* was reversed by ectopic expression of human Ada3, indicating that the loss of Ada3 itself, rather than alteration of any neighboring gene product, was responsible for the observed cell cycle phenotype.

Cell cycle progression is a tightly regulated process and is dependent on sequential and stringently controlled, concerted activation of Cdks and their inhibition by Cdk inhibitors. The novel cell cycle regulatory pathway downstream of Ada3 was suggested by our initial analyses of alterations in the levels of core components of mammalian cell cycle machinery. These analyses revealed a dramatic reduction in the key propeller of G_1/S phase transition, hypophosphorylated Rb when *Ada3* was deleted. Association of this defect with reduced Cdk2 activity without a reduction in Cdk2 levels suggested the role of elevated p27, which we established directly by demonstrating that shRNA knockdown of p27 substantially alleviated the G_1/S block imposed by Ada3 deficiency. Further biochemical connections were suggested by recent findings that STAGA complex, which includes Ada3 as a component, enhances c-*myc* transcription (32, 33). Because c-Myc is shown to regulate the transcription of *Skp2*, an essential component of the SCF(Skp2) cell cycle-associated E3 ligase that regulates p27 levels, we sought and established evidence that cell cycle-associated Myc transcription is Ada3-dependent and that Ada3 is required for *Skp2* transcription (which is a downstream target of Myc) and p27 stability (regulated by SCF(Skp2)). We provided direct evidence for key elements of this model, including ChIP analyses that demonstrated the cell cycle-associated early recruitment of Ada3 to c-*myc* enhancer elements. This result is consistent with independent findings from two groups that STAGA complex is recruited to c-Myc enhancer and regulates c-*myc* transcription (32, 33). In addition to control of c-*myc* gene transcription by Ada3-containing STAGA complex, studies have shown that STAGA associates with c-Myc on c-Myc target gene promoters and is required for efficient transcription activation by c-Myc (43, 44). This provides an additional mechanism by which Ada3 could control c-Myc-driven target genes that regulate cell proliferation. Thus, Ada3 might be involved in controlling both c-*myc* transcription as well as c-Myc function. Consistent with our observations, it is noteworthy that c-*myc* knock-out mice are embryonic lethal (45). Defective regulation of c-Myc transcription by Ada3-containing (STAGA or other) complexes might contribute to the early embryonic lethality seen in *Ada3*-null mice; further analyses of Myc-dependent pathways upon germline or conditional deletion of Ada3 during embryogenesis should help establish whether this is the case.

Although regulation of p27 protein stability by Ada3 through control of c-*myc* transcription forms an important basis for

G_1/S transition defects, we were not able to fully rescue the defect in cell cycle by using p27 shRNA, suggesting the involvement of other cellular pathways. To this end, examining global histone acetylations in *Ada3*-deficient cells revealed dramatic defects in histone acetylation. Because Ada3 forms a core structural component of various different HAT complexes in the cell, the presence of Ada3 is highly essential for structural maintenance and proper functioning of these complexes in cells. Additionally, loss of Ada3 led to substantial depletion of important HATs, p300, and PCAF proteins but not mRNA, which further explains the profound defects in histone acetylation seen upon loss of Ada3. This is consistent with the fact that PCAF and p300 are present in Ada3-containing protein complexes (8–11). These defects in histone acetylation could explain the partial rescue upon knockdown of p27 as histone acetylation has been shown to have an important role in the process of DNA replication (34, 35).

Given the role of Ada3 in regulating global histone acetylation and that histone acetylation is important in transcriptional activation of genes, we performed microarray analysis and showed that several genes were deregulated upon *Ada3* deletion. Analysis of these genes by ingenuity pathway analysis revealed the RNA post-transcriptional modification and cellular assembly and organization network as the top affected network, with the cell cycle, endocrine system development and function, and cancer network as the third most affected. The top network affected in the microarray data is consistent with an earlier study, which showed that Ada3-containing STAGA complex interacts with pre-mRNA splicing machinery, components suggesting a role for this complex in mRNA splicing (46). Importantly, the top biological functions affected upon deletion of *Ada3* included those involved in cell growth and proliferation with 386 deregulated genes involved in this process. Thus, our microarray data confirmed a role of Ada3 in cell cycle progression. Additionally, some of the top physiological functions affected upon deletion of Ada3 were those involving tissue development and organismal survival (supplemental Table S2), which could be linked to the early embryonic lethality observed upon knock-out of *Ada3* in mouse.

Notably, many of the genes that were involved in regulating cell growth and proliferation were those involved in mitosis and some that were involved in DNA replication. This led us to examine cell division upon deletion of *Ada3*. Consistent with the microarray data, we observed massive nuclear abnormalities, cell division defects, and delay in G_2/M to G_1 phase progression upon deletion of *Ada3*. Our observed phenomenon of cell division defects upon deletion of *Ada3* is consistent with a recently published study (14). The authors showed that ATAC HAT complex is specifically involved in regulating mitosis and that shRNA-mediated knockdown of Ada3 or Ada2a led to defects in cell division, which were attributed to stabilization of cyclin A upon disruption of ATAC complex. Although we did not observe an increase in cyclin A levels (in fact the converse) in our system, we did observe a similar effect on nuclear abnormalities and a clear defect in mitosis. Furthermore, the authors did not observe any changes in histone acetylation defects upon depletion of Ada3, which is not consistent with our results. Of note, Ada2a is a component of only ATAC complex; however,

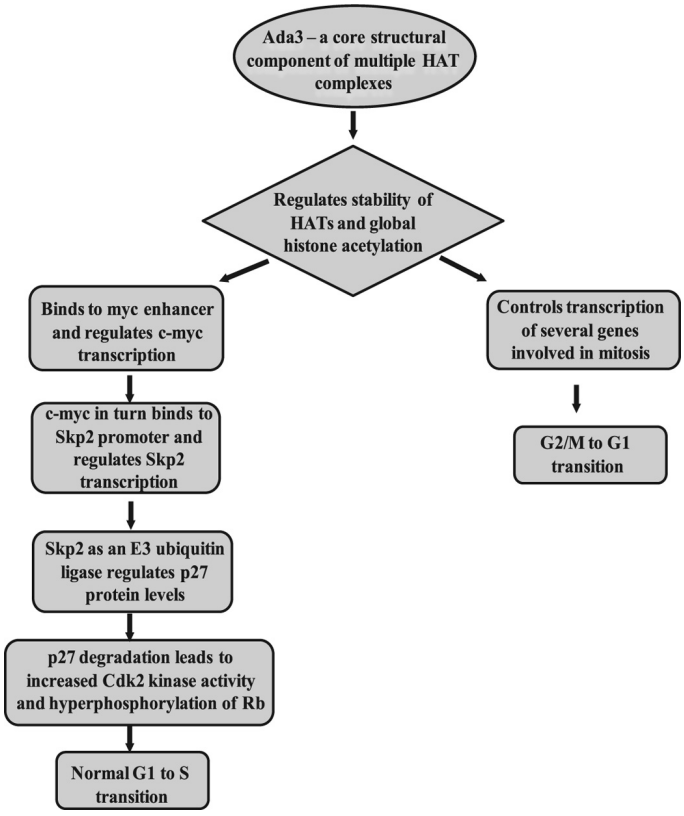

FIGURE 9. **Proposed model for the role of Ada3 in cell cycle progression.** As a core structural component of various HAT complexes, Ada3 maintains the integrity of HAT complexes and thus regulates global histone acetylation. Ada3 regulates G_1 to S transition by controlling transcription of c-*myc* gene, which in turn controls *Skp2* gene expression by binding to its promoter. Skp2 as an E3 ubiquitin ligase causes timely degradation of p27 protein so that cells can enter into S phase by increasing Cdk2 kinase activity, thus inducing hyperphosphorylation of Rb and cell progression from G_1 to S phase of cell cycle. Additionally, through controlling global histone acetylation, Ada3 controls transcription of various genes involved in cell division and is required for cells to undergo normal mitosis and G_2/M to G_1 progression.

Ada3 has been shown to be a core component of a number of HAT complexes. The authors used depletion of Ada3 as an indication of disruption of only ATAC complex; however, deletion of Ada3 would affect several HAT complexes and not just ATAC complex. Thus, deletion of *Ada3* would cause disruption of several HAT complexes that function in different phases of the cell cycle leading to defects in various phases of the cell cycle. Based on these findings, we propose the following working model of Ada3 regulation of cell cycle progression. As part of a chromatin-remodeling complex, likely the STAGA complex, Ada3 is recruited to and modifies the c-*myc* transcriptional regulatory elements to enhance *Skp2* transcription. This leads to destabilization of p27 by the SCF(Skp2) E3 ligase, resulting in increased Cdk2 activity and Rb phosphorylation to promote G_1/S progression. Additionally, Ada3, by regulating the number of genes involved in mitosis, regulates cell division. Lastly, Ada3 as part of ATAC and STAGA complex regulates transcription of various genes by recruiting HATs and acetylating histones. Combination of these functions led to severe cell cycle defect and embryonic lethality upon *Ada3* deletion (Fig. 9). Finally, although our studies here have focused on the role of Ada3 in cell cycle progression, future studies using cell type- or stage-specific condi-

tional deletion of *Ada3* in mouse to assess its role in functions other than transcriptional activation, including optimal transcription elongation, mRNA export, and nucleotide excision repair, need to be explored (8, 46, 47).

In conclusion, we demonstrate that the evolutionarily conserved Ada3 protein as an essential component of HAT complex plays an important role in embryogenesis and cell division. Thus, our studies identify Ada3 as a novel component of the physiological regulation of mammalian cell cycle progression and set the stage for future studies to assess the role of Ada3 in cell cycle progression during *in vivo* physiological and pathological settings. Use of $Ada3^{FL/FL}$ mice should facilitate these analyses to functionally dissect the *in vivo* roles of Ada3.

Acknowledgments—We acknowledge technical assistance from Valerie Tran and Poonam Joshi as well as assistance with time-lapse microscopy from Tom Dao. The University of Nebraska Medical Center (UNMC) DNA Microarray Core facility is supported by grants from the National Center for Research Resources (5P20RR016469) and the NIGMS (8P20GM103427), a component of the National Institutes of Health.

REFERENCES

1. Schafer, K. A. (1998) The cell cycle: a review. *Vet. Pathol* **35,** 461–478
2. Li, B., Carey, M., and Workman, J. L. (2007) The role of chromatin during transcription. *Cell* **128,** 707–719
3. Luger, K., Mäder, A. W., Richmond, R. K., Sargent, D. F., and Richmond, T. J. (1997) Crystal structure of the nucleosome core particle at 2.8 Å resolution. *Nature* **389,** 251–260
4. Kouzarides, T. (2007) Chromatin modifications and their function. *Cell* **128,** 693–705
5. Strahl, B. D., and Allis, C. D. (2000) The language of covalent histone modifications. *Nature* **403,** 41–45
6. Roth, S. Y., Denu, J. M., and Allis, C. D. (2001) Histone acetyltransferases. *Annu. Rev. Biochem.* **70,** 81–120
7. Carrozza, M. J., Utley, R. T., Workman, J. L., and Côté, J. (2003) The diverse functions of histone acetyltransferase complexes. *Trends Genet.* **19,** 321–329
8. Lee, K. K., and Workman, J. L. (2007) Histone acetyltransferase complexes: one size doesn't fit all. *Nat. Rev. Mol. Cell Biol.* **8,** 284–295
9. Nagy, Z., and Tora, L. (2007) Distinct GCN5/PCAF-containing complexes function as co-activators and are involved in transcription factor and global histone acetylation. *Oncogene* **26,** 5341–5357
10. Wang, T., Kobayashi, T., Takimoto, R., Denes, A. E., Snyder, E. L., el-Deiry, W. S., and Brachmann, R. K. (2001) hADA3 is required for p53 activity. *EMBO J.* **20,** 6404–6413
11. Germaniuk-Kurowska, A., Nag, A., Zhao, X., Dimri, M., Band, H., and Band, V. (2007) Ada3 requirement for HAT recruitment to estrogen receptors and estrogen-dependent breast cancer cell proliferation. *Cancer Res.* **67,** 11789–11797
12. Vernarecci, S., Ornaghi, P., Bâgu, A., Cundari, E., Ballario, P., and Filetici, P. (2008) Gcn5p plays an important role in centromere kinetochore function in budding yeast. *Mol. Cell. Biol.* **28,** 988–996
13. Paolinelli, R., Mendoza-Maldonado, R., Cereseto, A., and Giacca, M. (2009) Acetylation by GCN5 regulates CDC6 phosphorylation in the S phase of the cell cycle. *Nat. Struct. Mol. Biol.* **16,** 412–420
14. Orpinell, M., Fournier, M., Riss, A., Nagy, Z., Krebs, A. R., Frontini, M., and Tora, L. (2010) The ATAC acetyl transferase complex controls mitotic progression by targeting non-histone substrates. *EMBO J.* **29,** 2381–2394
15. Kumar, A., Zhao, Y., Meng, G., Zeng, M., Srinivasan, S., Delmolino, L. M., Gao, Q., Dimri, G., Weber, G. F., Wazer, D. E., Band, H., and Band, V. (2002) Human papillomavirus oncoprotein E6 inactivates the transcriptional coactivator human ADA3. *Mol. Cell. Biol.* **22,** 5801–5812
16. Piña, B., Berger, S., Marcus, G. A., Silverman, N., Agapite, J., and Guarente, L. (1993) ADA3: a gene, identified by resistance to GAL4-VP16, with properties similar to and different from those of ADA2. *Mol. Cell. Biol.* **13,** 5981–5989
17. Horiuchi, J., Silverman, N., Marcus, G. A., and Guarente, L. (1995) ADA3, a putative transcriptional adaptor, consists of two separable domains and interacts with ADA2 and GCN5 in a trimeric complex. *Mol. Cell. Biol.* **15,** 1203–1209
18. Saleh, A., Lang, V., Cook, R., and Brandl, C. J. (1997) Identification of native complexes containing the yeast coactivator/repressor proteins NGG1/ADA3 and ADA2. *J. Biol. Chem.* **272,** 5571–5578
19. Eberharter, A., Sterner, D. E., Schieltz, D., Hassan, A., Yates, J. R., 3rd, Berger, S. L., and Workman, J. L. (1999) The ADA complex is a distinct histone acetyltransferase complex in *Saccharomyces cerevisiae*. *Mol. Cell. Biol.* **19,** 6621–6631
20. Nag, A., Germaniuk-Kurowska, A., Dimri, M., Sassack, M. A., Gurumurthy, C. B., Gao, Q., Dimri, G., Band, H., and Band, V. (2007) An essential role of human Ada3 in p53 acetylation. *J. Biol. Chem.* **282,** 8812–8820
21. Zeng, M., Kumar, A., Meng, G., Gao, Q., Dimri, G., Wazer, D., Band, H., and Band, V. (2002) Human papilloma virus 16 E6 oncoprotein inhibits retinoic X receptor-mediated transactivation by targeting human ADA3 coactivator. *J. Biol. Chem.* **277,** 45611–45618
22. Zhao, Y., Lang, G., Ito, S., Bonnet, J., Metzger, E., Sawatsubashi, S., Suzuki, E., Le Guezennec, X., Stunnenberg, H. G., Krasnov, A., Georgieva, S. G., Schüle, R., Takeyama, K., Kato, S., Tora, L., and Devys, D. (2008) A TFTC/STAGA module mediates histone H2A and H2B deubiquitination, coactivates nuclear receptors, and counteracts heterochromatin silencing. *Mol Cell* **29,** 92–101
23. Todaro, G. J., and Green, H. (1963) Quantitative studies of the growth of mouse embryo cells in culture and their development into established lines. *J. Cell Biol.* **17,** 299–313
24. Weinberg, R. A. (1995) The retinoblastoma protein and cell cycle control. *Cell* **81,** 323–330
25. Dyson, N. (1998) The regulation of E2F by pRB family proteins. *Genes Dev.* **12,** 2245–2262
26. Nourse, J., Firpo, E., Flanagan, W. M., Coats, S., Polyak, K., Lee, M. H., Massague, J., Crabtree, G. R., and Roberts, J. M. (1994) Interleukin-2-mediated elimination of the $p27^{Kip1}$ cyclin-dependent kinase inhibitor prevented by rapamycin. *Nature* **372,** 570–573
27. Reynisdóttir, I., Polyak, K., Iavarone, A., and Massagué, J. (1995) Kip/Cip and Ink4 Cdk inhibitors cooperate to induce cell cycle arrest in response to TGF-β. *Genes Dev.* **9,** 1831–1845
28. Sherr, C. J., and Roberts, J. M. (1999) CDK inhibitors: positive and negative regulators of G_1 phase progression. *Genes Dev.* **13,** 1501–1512
29. Besson, A., Gurian-West, M., Chen, X., Kelly-Spratt, K. S., Kemp, C. J., and Roberts, J. M. (2006) A pathway in quiescent cells that controls $p27^{Kip1}$ stability, subcellular localization, and tumor suppression. *Genes Dev.* **20,** 47–64
30. Carrano, A. C., Eytan, E., Hershko, A., and Pagano, M. (1999) SKP2 is required for ubiquitin-mediated degradation of the CDK inhibitor p27. *Nat. Cell Biol.* **1,** 193–199
31. Bretones, G., Acosta, J. C., Caraballo, J. M., Ferrándiz, N., Gómez-Casares, M. T., Albajar, M., Blanco, R., Ruiz, P., Hung, W. C., Albero, M. P., Perez-Roger, I., and León, J. (2011) SKP2 oncogene is a direct MYC target gene, and MYC down-regulates p27(KIP1) through SKP2 in human leukemia cells. *J. Biol. Chem.* **286,** 9815–9825
32. Chen, J., Luo, Q., Yuan, Y., Huang, X., Cai, W., Li, C., Wei, T., Zhang, L., Yang, M., Liu, Q., Ye, G., Dai, X., and Li, B. (2010) Pygo2 associates with MLL2 histone methyltransferase and GCN5 histone acetyltransferase complexes to augment Wnt target gene expression and breast cancer stem-like cell expansion. *Mol. Cell. Biol.* **30,** 5621–5635
33. Yang, M., Waterman, M. L., and Brachmann, R. K. (2008) hADA2a and hADA3 are required for acetylation, transcriptional activity, and proliferative effects of β-catenin. *Cancer Biol. Ther.* **7,** 120–128
34. Bhaskara, S., Chyla, B. J., Amann, J. M., Knutson, S. K., Cortez, D., Sun, Z. W., and Hiebert, S. W. (2008) Deletion of histone deacetylase 3 reveals critical roles in S phase progression and DNA damage control. *Mol. Cell*

30, 61–72
35. Burgess, R. J., Zhou, H., Han, J., and Zhang, Z. (2010) A role for Gcn5 in replication-coupled nucleosome assembly. *Mol. Cell* **37,** 469–480
36. Grau, B., Popescu, C., Torroja, L., Ortuño-Sahagún, D., Boros, I., and Ferrús, A. (2008) Transcriptional adaptor ADA3 of *Drosophila melanogaster* is required for histone modification, position effect variegation, and transcription. *Mol. Cell. Biol.* **28,** 376–385
37. Ciemerych, M. A., and Sicinski, P. (2005) Cell cycle in mouse development. *Oncogene* **24,** 2877–2898
38. Yao, T. P., Oh, S. P., Fuchs, M., Zhou, N. D., Ch'ng, L. E., Newsome, D., Bronson, R. T., Li, E., Livingston, D. M., and Eckner, R. (1998) Gene dosage-dependent embryonic development and proliferation defects in mice lacking the transcriptional integrator p300. *Cell* **93,** 361–372
39. Yamauchi, T., Yamauchi, J., Kuwata, T., Tamura, T., Yamashita, T., Bae, N., Westphal, H., Ozato, K., and Nakatani, Y. (2000) Distinct but overlapping roles of histone acetylase PCAF and of the closely related PCAF-B/GCN5 in mouse embryogenesis. *Proc. Natl. Acad. Sci. U.S.A.* **97,** 11303–11306
40. Kasper, L. H., Fukuyama, T., Biesen, M. A., Boussouar, F., Tong, C., de Pauw, A., Murray, P. J., van Deursen, J. M., and Brindle, P. K. (2006) Conditional knockout mice reveal distinct functions for the global transcriptional coactivators CBP and p300 in T-cell development. *Mol. Cell. Biol.* **26,** 789–809
41. Guelman, S., Kozuka, K., Mao, Y., Pham, V., Solloway, M. J., Wang, J., Wu, J., Lill, J. R., and Zha, J. (2009) The double-histone-acetyltransferase complex ATAC is essential for mammalian development. *Mol. Cell. Biol.* **29,** 1176–1188
42. Herceg, Z., Hulla, W., Gell, D., Cuenin, C., Lleonart, M., Jackson, S., and Wang, Z. Q. (2001) Disruption of Trrap causes early embryonic lethality and defects in cell cycle progression. *Nat. Genet.* **29,** 206–211
43. Liu, X., Tesfai, J., Evrard, Y. A., Dent, S. Y., and Martinez, E. (2003) c-Myc transformation domain recruits the human STAGA complex and requires TRRAP and GCN5 acetylase activity for transcription activation. *J. Biol. Chem.* **278,** 20405–20412
44. Liu, X., Vorontchikhina, M., Wang, Y. L., Faiola, F., and Martinez, E. (2008) STAGA recruits Mediator to the MYC oncoprotein to stimulate transcription and cell proliferation. *Mol. Cell. Biol.* **28,** 108–121
45. Davis, A. C., Wims, M., Spotts, G. D., Hann, S. R., and Bradley, A. (1993) A null c-*myc* mutation causes lethality before 10.5 days of gestation in homozygotes and reduced fertility in heterozygous female mice. *Genes Dev.* **7,** 671–682
46. Martinez, E., Palhan, V. B., Tjernberg, A., Lymar, E. S., Gamper, A. M., Kundu, T. K., Chait, B. T., and Roeder, R. G. (2001) Human STAGA complex is a chromatin-acetylating transcription coactivator that interacts with pre-mRNA splicing and DNA damage-binding factors *in vivo*. *Mol. Cell. Biol.* **21,** 6782–6795
47. Torok, M. S., and Grant, P. A. (2004) Histone acetyltransferase proteins contribute to transcriptional processes at multiple levels. *Adv. Protein Chem.* **67,** 181–199

SUPPLEMENTARY MATERIALS AND METHODS:

Generation of conditional Ada3 knockout targeting construct-To generate a conditional targeting construct, we examined the genomic structure of the mouse Ada3 gene. According to the NCBI mouse genome resources (Build 32.1), mouse Ada3 gene is located on chromosome 6, is composed of 9 exons and spans approximately 11kb. We flanked exons 2 to 4 with loxP sequences so that these exons can be removed from the chromosome using Cre-dependent recombination. Exons 2 to 4 were targeted based on the following considerations. Targeting of these three exons will lead to deletion of 188 amino acids amounting to about 43% of protein coding sequence and the transcript from the remaining exons is unlikely to lead to a functional protein product. Limiting the gene manipulation to exons 2 to 4 also minimized potential effects on promoter/enhancer elements of neighboring genes (**http://www.ncbi.nlm.nih.gov/entrez/query.fcgi?db=gene&cmd=Retrieve&dopt=Graphics&list_uids=70601**). We used a probe from Ada3 genomic region to screen a BAC library (RPCI-22 (129S6/SvEvTac) (Children's Hospital Oakland Research Institute, bacpac.chori.org) and identified a clone that had the required genomic region of Ada3 locus to generate a targeting construct. LoxP sites were introduced using a recombineering technique, as previously described (1).

Generation of Ada3 gene-targeted mice and isolation of mouse embryos and PCR genotyping-A duplex-PCR based strategy was developed to distinguish between the wild-type and Ada3 mutant alleles. The primers are as follows: a, 5'-CGGGAGGGGGAGCTCTATGAATCCTGATCTAT-3'; b, 5'-TCAACATAATTTCTCTGTATAACAACTCTGGC-3'; c, 5'- CAATATGACTAACTACATCTCTGG-3' (Supplementary Figure S1A). A 470-bp fragment indicates the presence of the wild type allele, whereas a 703-bp fragment is amplified from the mutated allele. For analysis of post implantation embryos, *Ada3*$^{+/-}$ females were sacrificed at various time points (see Table 1) after being mated to *Ada3*$^{+/-}$ males. Embryos were dissected from the uteri and washed in phosphate-buffered saline (PBS), and DNA was isolated after proteinase K (Roche) digestion. Genotyping was performed by a duplex PCR using the duplex-PCR mentioned above. For blastocyst isolation, plugged *Ada3*$^{+/-}$ females were euthanized at 3.5 dpc, and their uteri were dissected and flushed with DMEM. Blastocysts were either directly genotyped or seeded singly onto 24-well plates and cultured in complete DMEM at 37°C with 5% CO_2. After 4 days, the medium was changed, and after 7 days in culture, blastocyst DNA was isolated and subjected to genotyping PCR

Generation of Ada3 monoclonal antibody and Immunoblotting-Full length human Ada3 cDNA was cloned into pGEX 6P1 bacterial expression vector (that contain N-terminal GST tag followed by a precision protein). The recombinant protein (hAda3) was purified from a large scale culture of BL21 *E. coli* using Glutathione Sepharose 4B beads (Pharmacia). GST tag was cleaved using Precision protease and purified hAda3 was used as an antigen to produce monoclonal antibodies at the Monoclonal Antibody Core Facility, Lurie Cancer Center, Northwestern University, Chicago. The clones were screened by i) western blotting using 293T cell lysates as an endogenous Ada3 and using flag-tagged Ada3 overexpressing 293T cell lysates and also by ii) immunoprecipitation of endogenous or exogenous Ada3 from 293T cell lysates (data not shown). A few well reacting antibodies were selected among which the clone 5C9/C8 was used for subsequent experiments. Clone 5C9/C8 recognized a single band of estimated size in western blotting and immunoprecipitation. This clone was used for immunoblotting experiments conducted in the paper. Other primary antibodies used to perform immunoblotting were Rb (554136, Pharmingen); Cyclin A (sc-596), Cyclin E (sc-481), Cyclin D1 (sc-20044), Cdk2 (sc-6248), Cdk4 (sc-260), Cdk6 (sc-53638), p27 (sc-1641), p21 (sc-6246), p16 (sc-1661), p300 (sc-585), PCAF (sc-15124) and Hsc-70 (sc-7298) (Santa Cruz Biotechnology, Santa Cruz, CA); c-myc (1472-1, Epitomics); H2B-K5 (07-382), H2B (05-1352), H3 (06-755), H3-K9 (07-352), H3-K56 (07-677) and H4 (05-858) (Millipore); histone Ab sampler kit (H2A-K5, H2A, H2B-K5, H3-K9, H4-K8) (9933, Cell Signaling) and β-actin (A5441, Sigma).

Generation of recombinant baculoviruses and Ada3-His expression using Bac-to-Bac® Expression System-Ada3 coding sequence was PCR amplified to contain 6X Histidine tag in the C-terminus and cloned into (SalI and NotI Sites) of pFastBac™ donor plasmid and

the recombinant baculovirus expressing Ada3-His protein was produced following manufacturer's instructions. Sf21 cells infected with recombinant baculovirus were lysed and the Ada3-His protein was purified using Ni-NTA column.

HAT assay-HAT assays were carried out in buffer containing 50 mM Tris HCl pH 8.0, 50 mM KCl, 5% glycerol, 0.1 mM EDTA, 1mM DTT, 10mM sodium butyrate, [^{3}H] Acetyl Coenzyme-A (Perkin-Elmer) and 1mM PMSF at 30°C using core histones or histone H3 alone as a substrate. Recombinant p300 catalytic domain was purchased from Active Motif. Purified core histones from chicken erthyrocytes were purchased from Upstate and purified. Histone H3 from calf thymus was purchased from Roche. Briefly, 10ng of p300 catalytic domain was incubated with varying concentrations of purified baculoviral Ada3 and either 1 ug of core histones or 1 ug of Histone H3 in HAT buffer for 15 min. The products were subjected to SDS-PAGE, transferred to PVDF membranes, and autoradiographed. The PVDF membranes were sprayed with EN^{3}HANCE spray (Perkin Elmer) to enhance the signals from tritium prior to autoradiography.

Microarray analyses-Three days after infecting *Ada3*$^{FL/FL}$ MEFs with Ctrl and Cre Adenoviruses, total RNA was isolated using the TRIzol reagent. Biotin labeled cRNA was generated from 200 ng of total RNA using the Ambion WT Expression Kit (Ambion) per manufacturer's instructions. Hybridization, scanning of the chip and initial scaling was performed as previously described (2); except that Affymetrix GeneChip Mouse Genome 430 2.0 Array was used for cRNA hybridization. Intensities were imported into Affymetrix Expression console software using Robust Multi-chip Averaging (RMA) background correction and fold-change differences between samples were determined. Microarray analysis was performed using duplicate samples and the values represent average of the two independent experiments.

Time Lapse Microscopy-24 h after control and Cre adenovirus infection, *Ada3*$^{FL/FL}$ MEFs were plated in 6 well plates at 30% confluency. One day after plating, cells were placed on a robotized stage of an Olympus IX81 DSU Spinning Disk confocal microscope equipped with a chamber maintained at 37^o C with 5% CO_2. Movies were acquired over 24 h (10 min intervals) using Hamamatsu ORCA-ERG camera and automated acquisition software (Slidebook Software) at 10x magnification.

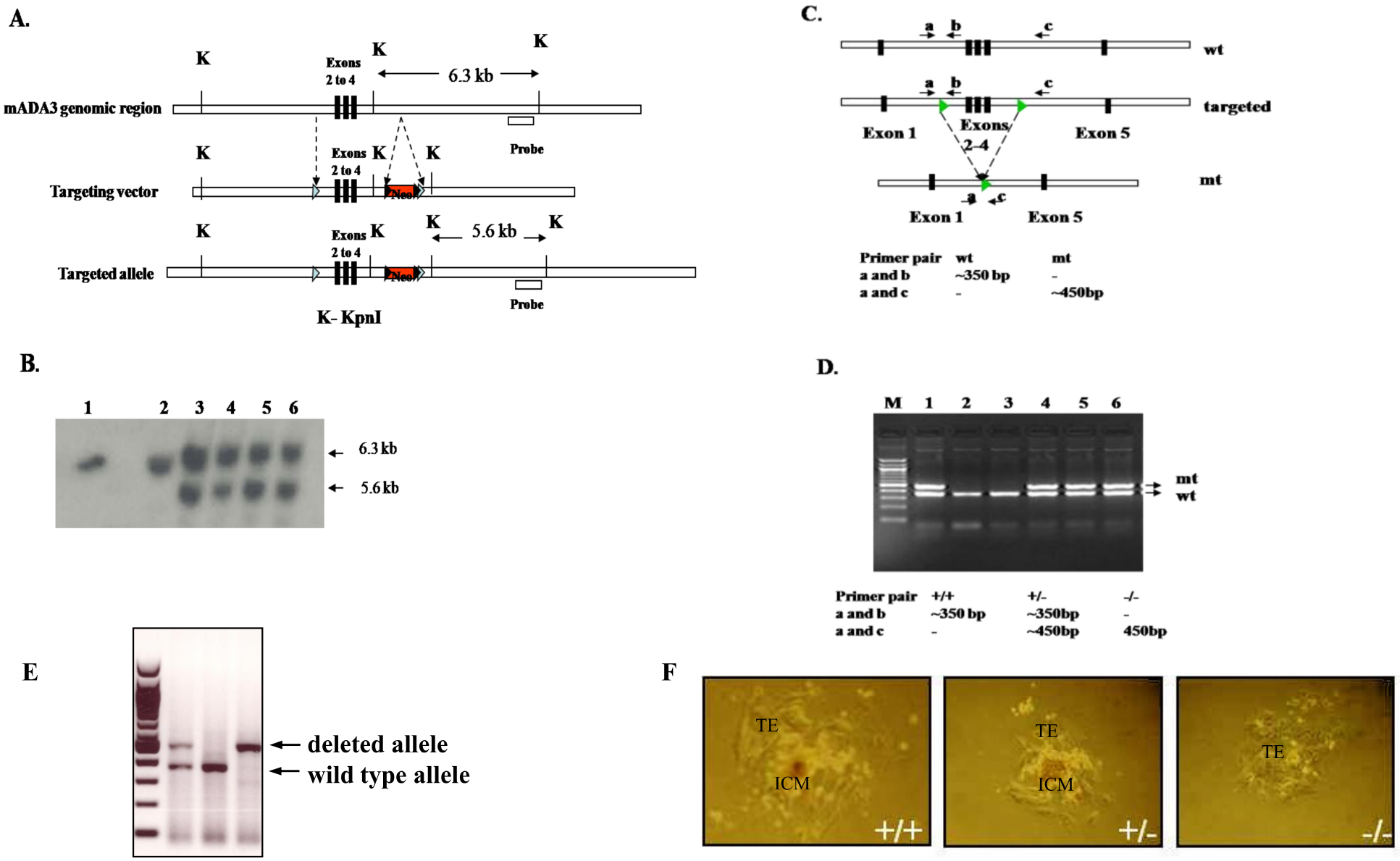

Supplementary Figure S1. **Targeting of *mAda3* locus and PCR genotyping strategy.** (A) Schematic representation of the targeting strategy used to disrupt *mAda3*. (B) Southern blotting of DNA from ES cell clones digested with KpnI and probed with *Ada3* locus specific probe; lanes 3-6 represent positive clones; lanes 1 and 2 represent wild type. (C) PCR strategy to screen for the deleted allele. (D) A representative gel picture showing genotyping of a litter from $Ada3^{+/-}$ intercross. (E) Blastocysts isolated from 3.5 day post coitus from $Ada3^{+/-}$ females mated with $Ada3^{+/-}$ males were cultured in DMEM with 10% fetal calf serum for 7 days and the cells recovered from blastocyst outgrowth were subjected to genotyping PCR. A representative gel image showing PCR results of blasocyst outgrowths. (F) Representative microscopic images showing each of the three Ada3 genotype blastocysts. ICM, inner cell mass; TE, trophectoderm

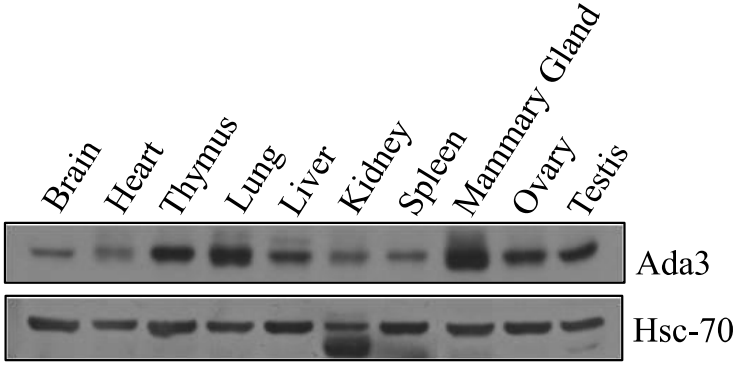

Supplementary Figure S2. Analysis of Ada3 protein levels in mouse tissues. Protein lysates obtained from various tissues of an adult wild type mouse were subjected to immunoblotting to determine the expression levels of Ada3 protein.

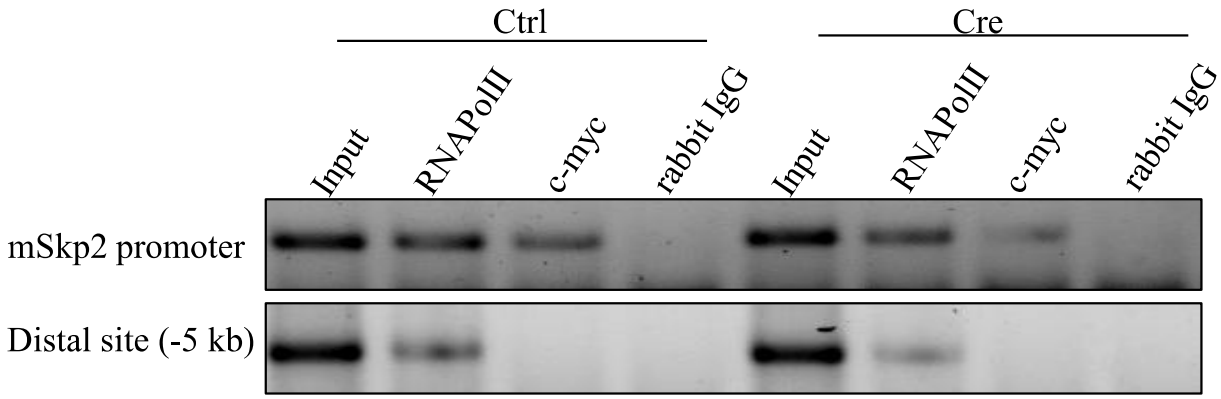

Supplementary Figure S3. Skp2 promoter occupancy by c-myc is reduced upon deletion of Ada3. Chromatin fragments from asynchronous control (Ctrl) and Cre *Ada3*$^{FL/FL}$ MEFs cells were immunoprecipitated with anti c-myc antibody. The immunoprecipitated DNA was analyzed by PCR, using mouse Skp2 promoter specific primers. Primers amplifying a region that is 5 kb upstream of the mouse Skp2 promoter were used as a negative control.

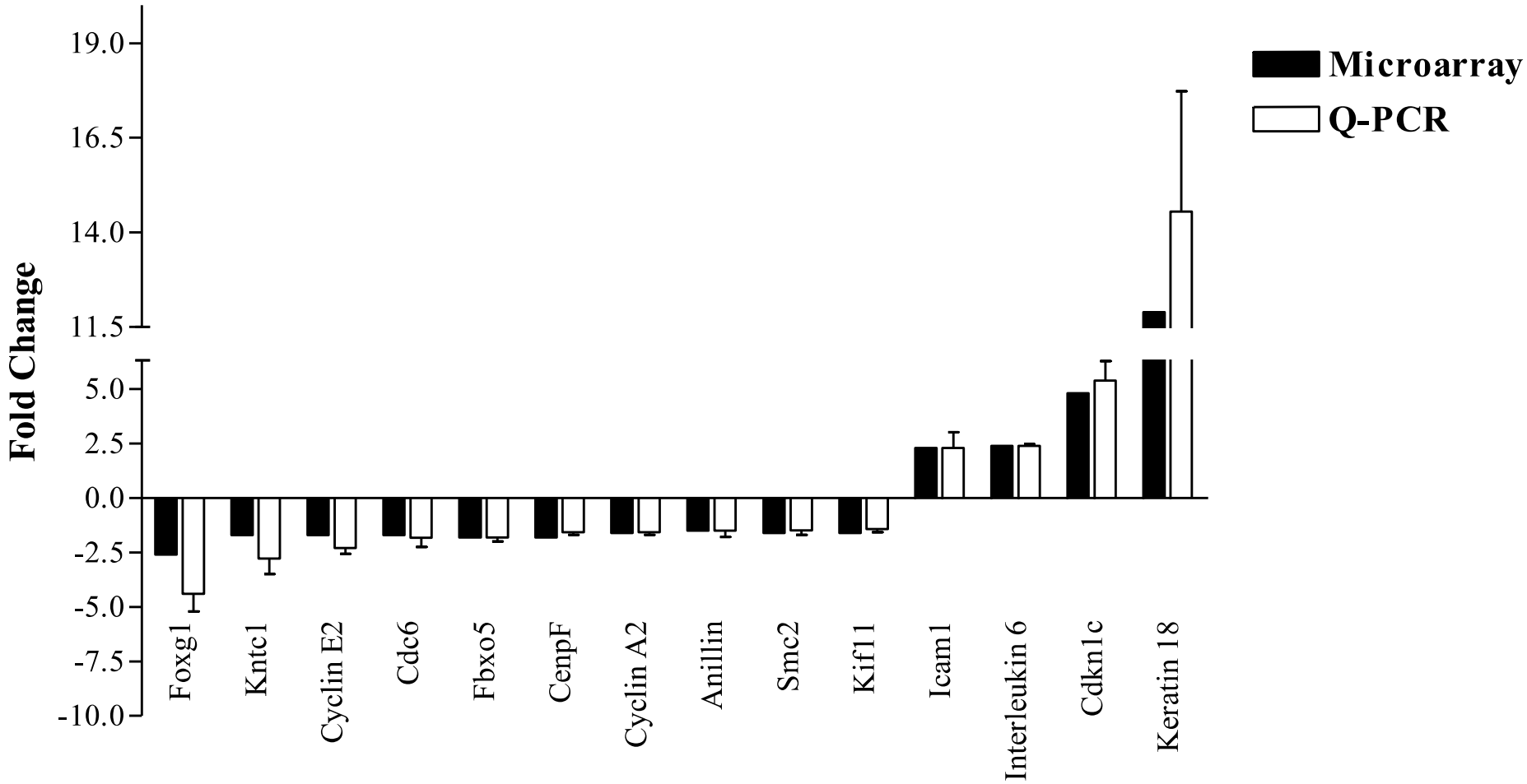

Supplementary Figure S4. Validation of microarray analysis by q-RT-PCR. Microarray data from Ctrl and Cre infected MEFs was verified by qRT-PCR by picking several deregulated genes from microarray. Error bars indicate mean ± S.E. from three independent experiments.

A

Network 1: RNA Post-Transcriptional Modification, Cellular Assembly and Organization, Gastrointestinal Disease

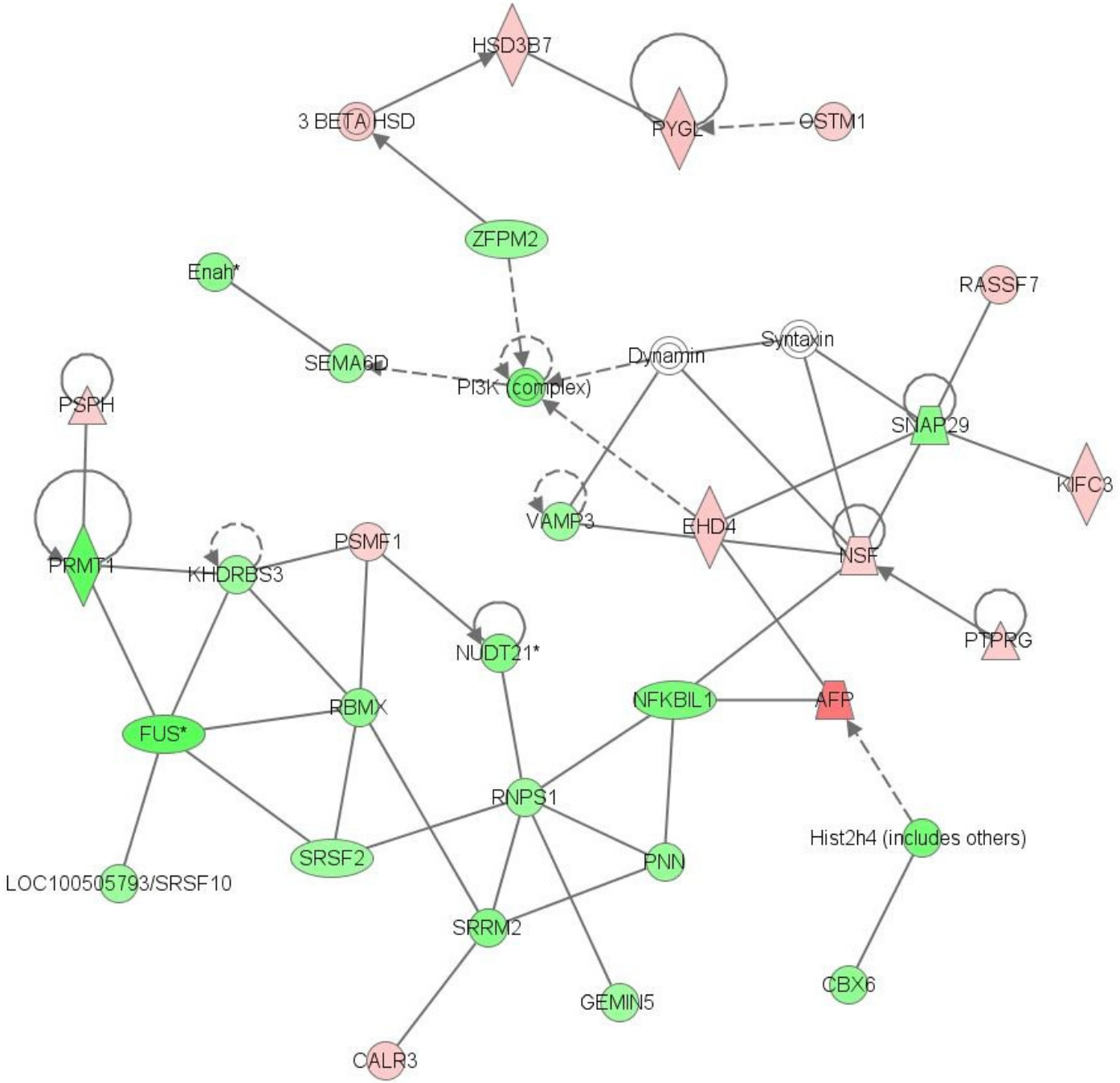

B

Network 2: Cellular Function and Maintenance, Molecular Transport, Cell Death

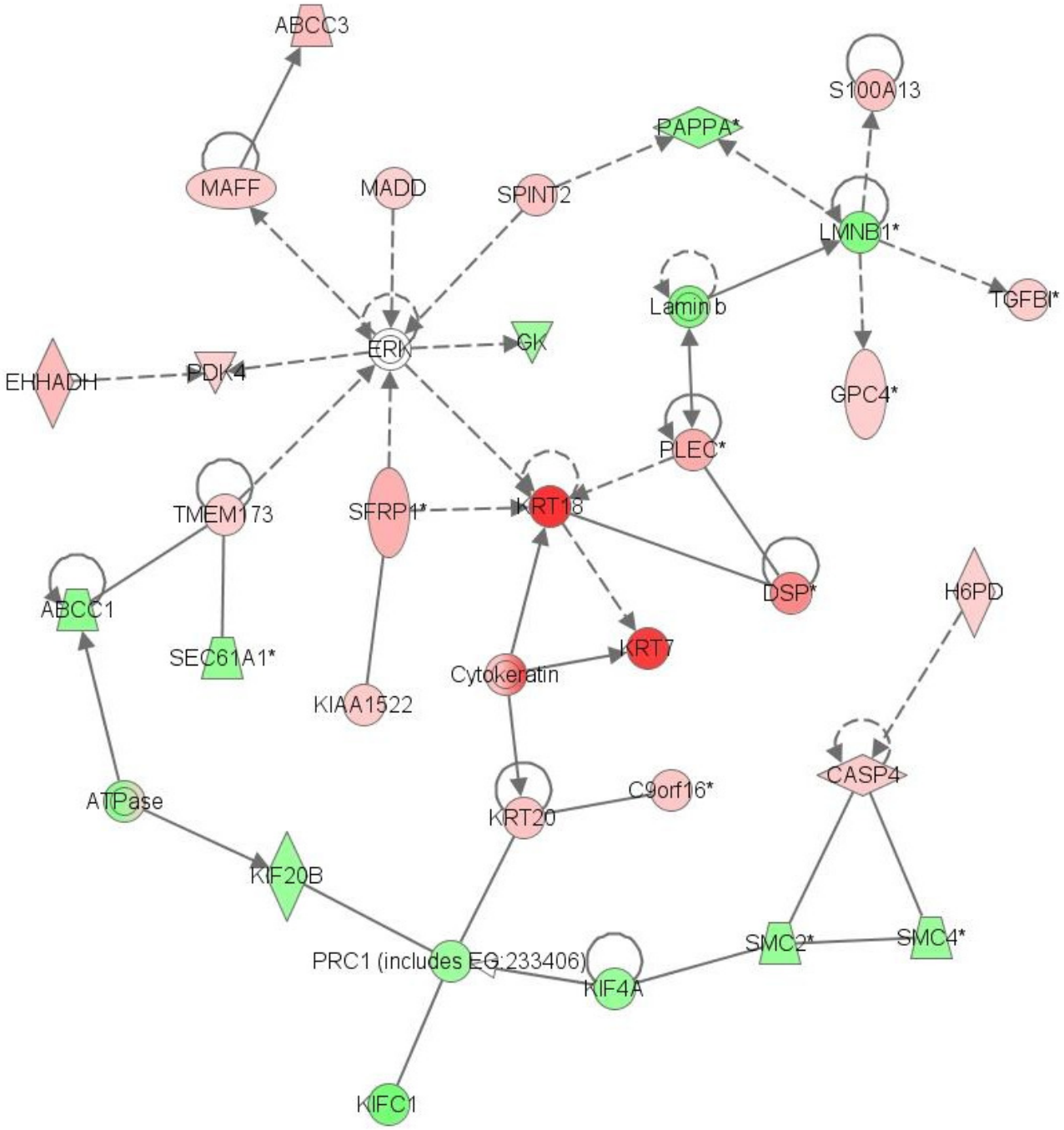

C

Network 3: Cell Cycle, Endocrine System Development and Function, Cancer

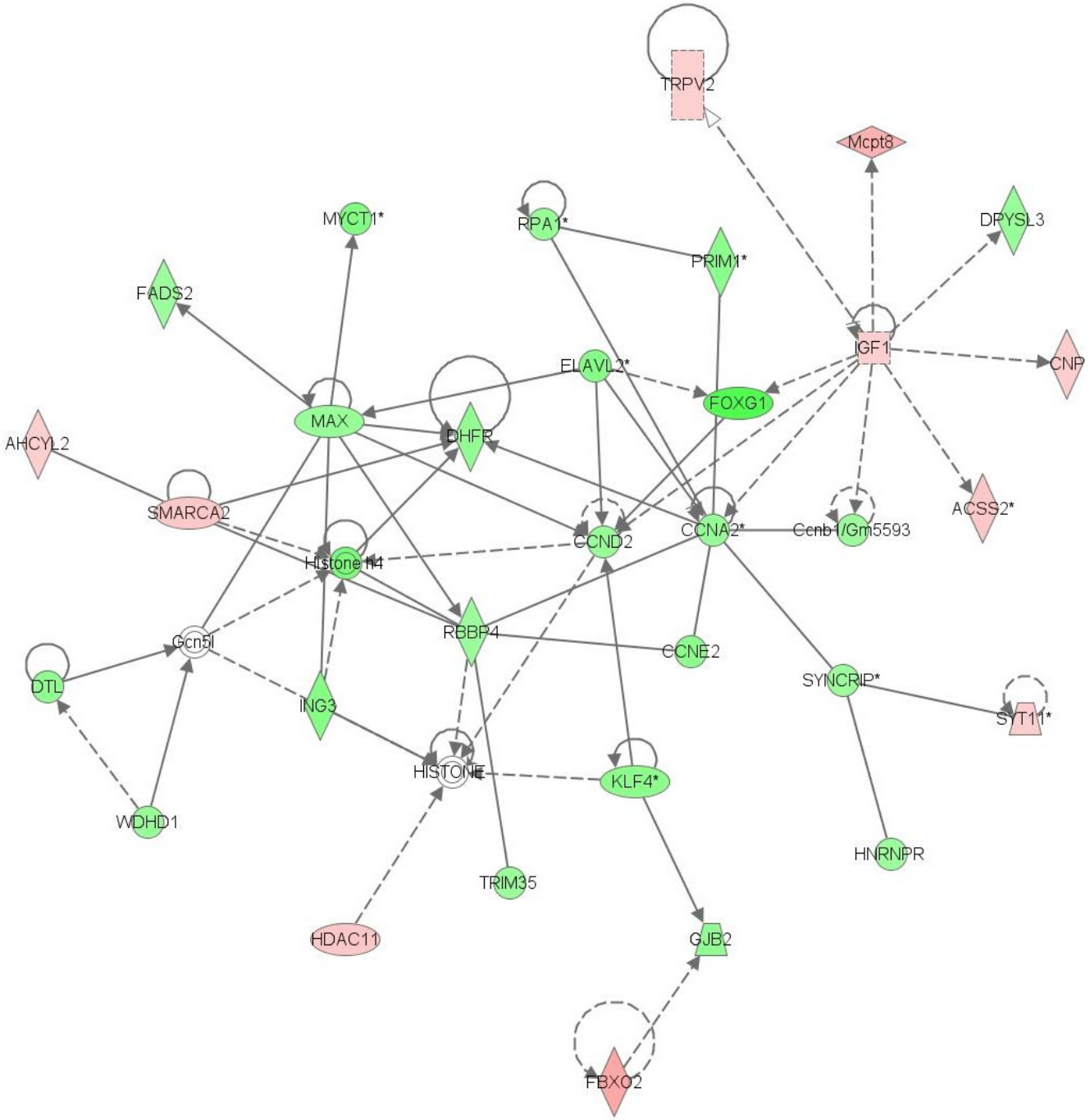

D

Network 4: Lipid Metabolism, Small Molecule Biochemistry, Cell Death

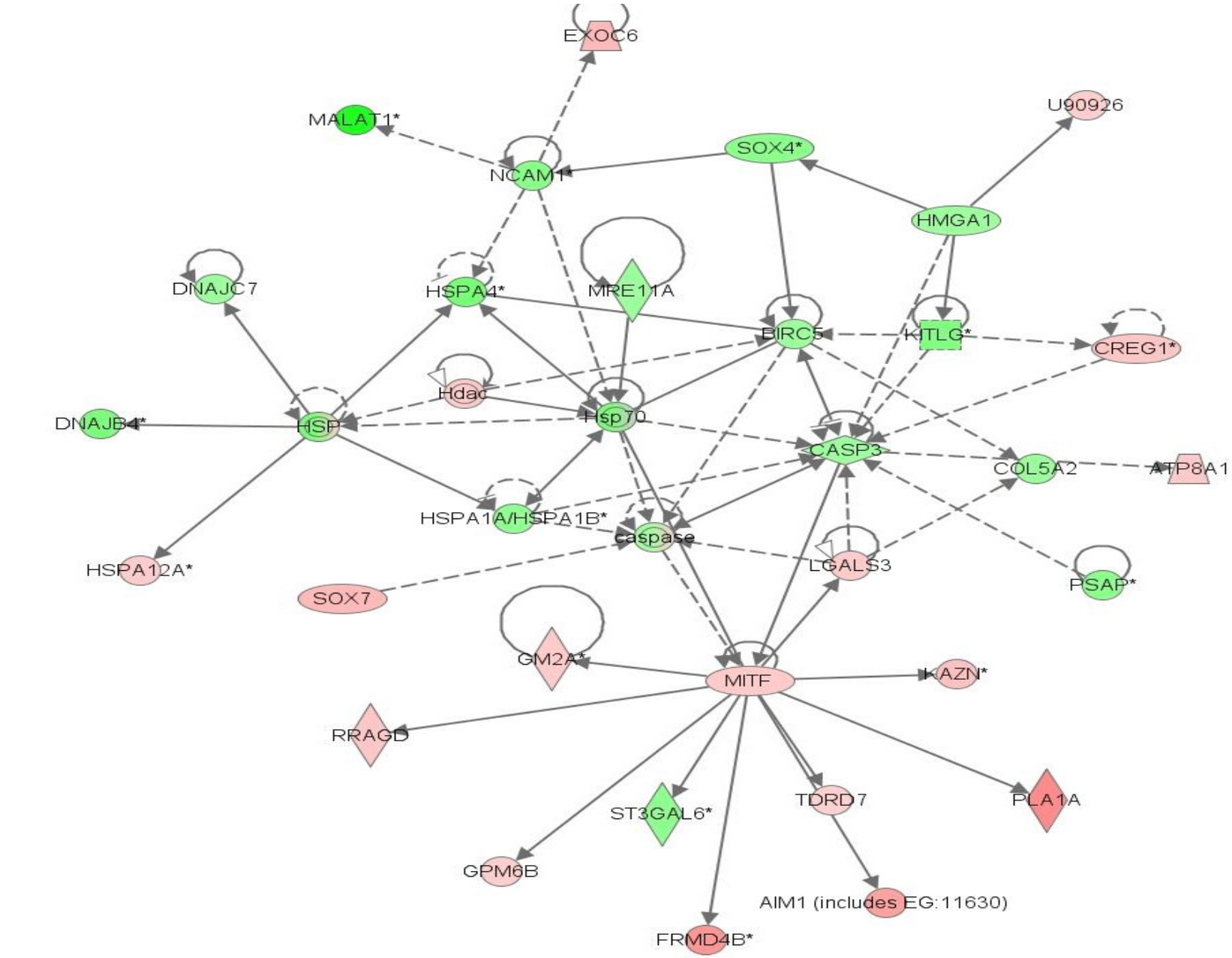

E

Network 5: Cell Cycle, Cellular Assembly and Organization, DNA Replication, Recombination, and Repair

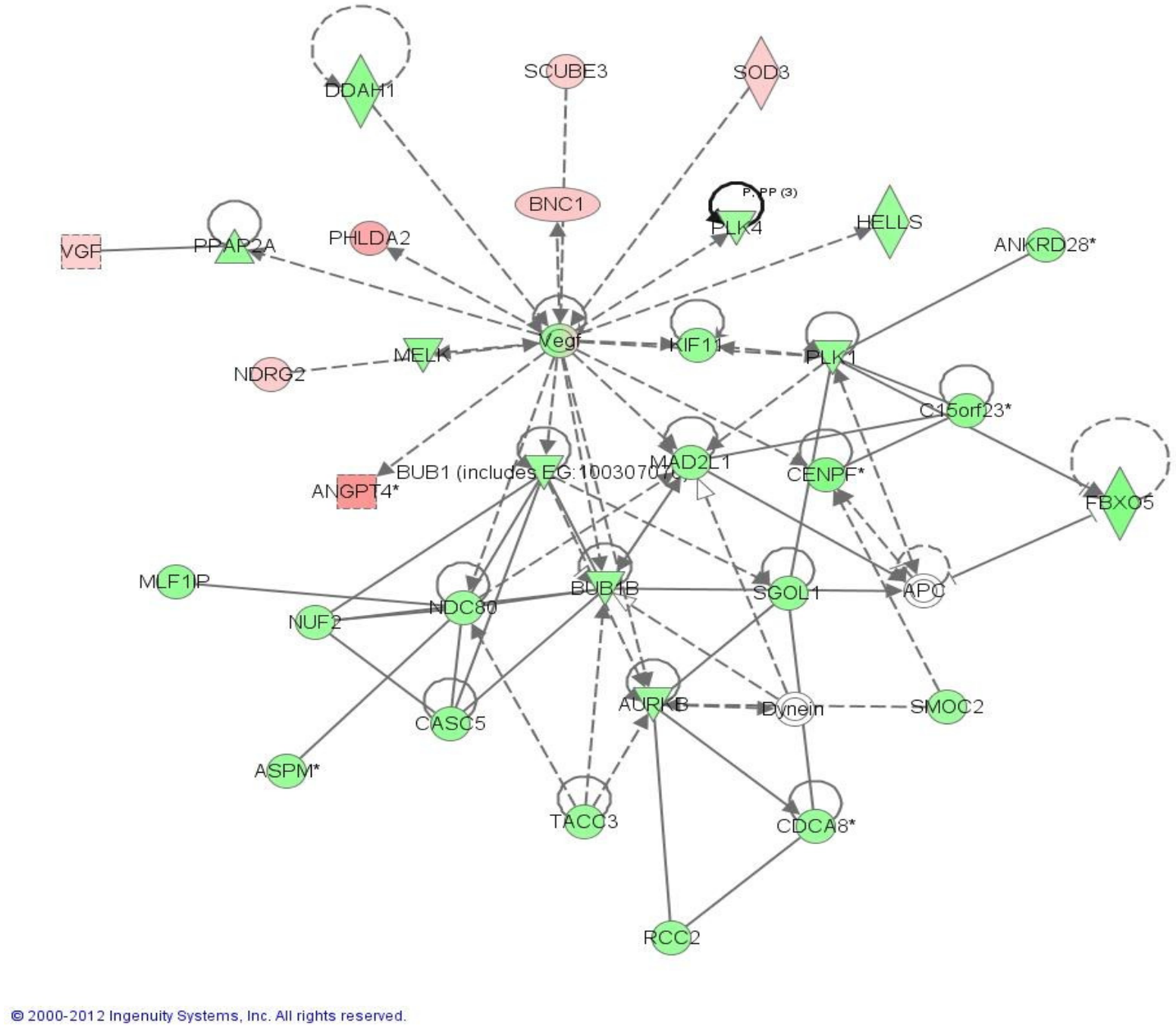

Supplementary Figure S5. Ingenuity Pathway Analysis. (A-E) Top 5 networks affected upon Ada3 deletion as obtained by Ingenuity pathway analysis. All the genes that were induced or downregulated at least 1.5 fold were used for the analysis

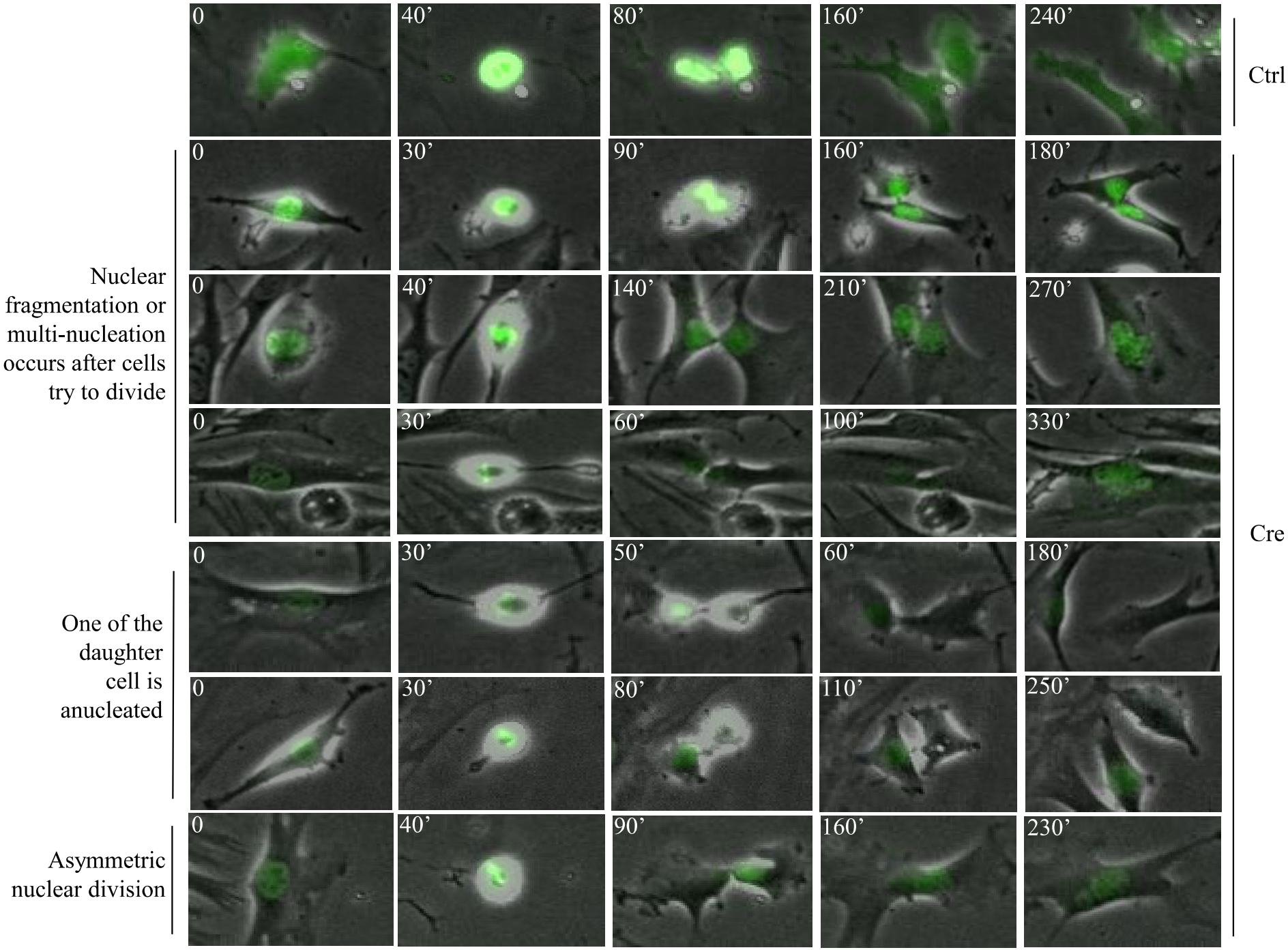

Supplementary Figure S6. Abnormal cell division of Ada3 deleted cells. Representative time lapse images of *Ada3*$^{FL/FL}$ cells after 2 days of infection with control (Ctrl) or Cre adenovirus captured over 24 hours period. Note that cells infected with control virus express eGFP in both cytoplasm and nucleus whereas expression of eGFP in Cre infected cells is restricted to the nucleus. Figures in the upper left hand corner of each image indicate minutes.

Supplemental Table S1: Deregulated genes in Ada3-deleted cells

Gene Symbol	Representative Public ID	Fold change
Downregulated genes		
Hmox1	NM_010442	5.4
Cdkn2a	NM_009877	4.5
Gsta1 /// Gsta2	NM_008182	4.3
Malat1	AW012617	3.9
Ptprz1	BC002298	3.4
Ptprz1	BC002298	3.2
LOC639633 /// Npm3 /// Npm3-ps1	BB811478	2.7
Foxg1	NM_008241	2.6
Stmn2	BM115022	2.6
Mex3b	BG072837	2.5
Fus	AF224264	2.5
Vcan	BM251152	2.4
Fam171a2	BB452429	2.4
Cd80	X60958	2.4
Prmt1	AK020120	2.4
3110039M20Rik	AW494150	2.4
Rian	AK017440	2.3
Ptk7	AK018379	2.3
Psma3	C77757	2.3
LOC100047441 /// Msl1	AW495537	2.3
Zc3h7b	BM125518	2.3
Gpr124	NM_054044	2.3
Dok1	BC013066	2.2
Rtn4	NM_024226	2.2
Vip	AK018599	2.2
Pik3r1	M60651	2.1
Mmp14	BB535404	2.1
Plec1	BM232239	2.1
Mgp	NM_008597	2.1
Rad18	AK012795	2.1
2310076G05Rik	BB197581	2.1
Fgf13	AF020737	2.1
Setd5	BI739725	2.1
Nrk	AK012873	2.1
Gja1	M63801	2.1
Mycl1	BG064871	2.1
Tcfec	NM_031198	2.1
Prl8a9	AF158744	2.1

Hspa4	BE912771	2.1
6030442H21Rik	AK020062	2.1
Stxbp6	BC024598	2.1
Col11a1	NM_007729	2.0
Kifc1 /// LOC100044746	NM_016761	2.0
Plau	NM_008873	2.0
2210411K19Rik	BI694945	2.0
Gas7	AI506234	2.0
Cdc42ep3	BB012489	2.0
Rab5c	BC023027	2.0
Dhrs3	NM_011303	2.0
Pip5k1a	BC003763	2.0
A630033H20Rik	BB034567	2.0
Nfkbil1	NM_010909	2.0
Cdc42ep3	BB012489	2.0
Cd34	NM_133654	2.0
Arpc3	BC013618	2.0
Col11a1	NM_007729	2.0
Dnajb4	AK006478	2.0
LOC100047441 /// Msl1	AW495537	2.0
Epha3	AV226618	2.0
Cxcr7	BC015254	2.0
D330050I23Rik	BE303700	2.0
Grb14	NM_016719	2.0
Plau	NM_008873	1.9
D17H6S56E-5	NM_033075	1.9
D17H6S56E-5	NM_033075	1.9
Pik3r1	BB426164	1.9
Lce1h	NM_026335	1.9
Kitl	BB815530	1.9
Adra2a	BB262415	1.9
Sema3a	NM_009152	1.9
C530008M17Rik	BB493717	1.9
S1pr1	BB133079	1.9
Atp2b1	BI080417	1.9
Adamts6	BB227648	1.9
Thoc3	BE335845	1.9
Myct1	AI642973	1.9
Arl2bp	NM_024191	1.9
Stmn2	BM115022	1.9
Kitl	BB815530	1.9
Epha7	BC026153	1.9
Tmem35	NM_026239	1.9

Cd80	AK019867	1.9
2210411K19Rik /// Rpl41	BI694945	1.9
Stom	AF093620	1.9
Slfn9	BI647893	1.9
Blnk	AF068182	1.9
Ptchd1	BB271066	1.9
Samd4	BF319665	1.9
Lpar4	AW493905	1.9
Lmnb1	AA270173	1.9
Aldh1a1	NM_013467	1.9
4921513D23Rik	AV254721	1.9
C130021I20Rik	AW209204	1.9
Rnf25	NM_021313	1.8
Itgbl1	BC020152	1.8
Dbc1	AB060589	1.8
Hmgb3	NM_008253	1.8
Fbxo5	AK011820	1.8
Rlf	BF020283	1.8
Jun	NM_010591	1.8
Unc5c	NM_009472	1.8
LOC100046744 /// Srrm2	BQ176063	1.8
Tnfrsf11b	AB013898	1.8
5430416N02Rik	AW112059	1.8
Arl2bp	AK006418	1.8
Slc20a2	BG144370	1.8
Elavl2	BB105998	1.8
Gap43	BB622036	1.8
Cenpf	BE848253	1.8
Ing3	BB020556	1.8
Nudt21	BG070110	1.8
Edil3	BB377340	1.8
Slc8a1	BB313689	1.8
Hipk2	AF170301	1.8
Maoa	AW986246	1.8
OTTMUSG00000015563	AK013448	1.8
9830001H06Rik	BB093445	1.8
Arf6	BI248938	1.8
Dhcr24	BG295389	1.8
Alg8	BM249614	1.8
Snap29	BF682880	1.8
Fam110c	NM_027828	1.8
Lpar4	BB417145	1.8
Ncam1	BM201198	1.8

Lpar4	BB297502	1.8
Tbx20	AK020409	1.8
Myct1	W34301	1.8
Npy1r	NM_010934	1.8
Sprr2k	NM_011477	1.7
Klf4	BG069413	1.7
Cenpf	BB667318	1.7
Gpr149	BB126999	1.7
D430042O09Rik	BB486367	1.7
Galntl4	AV238718	1.7
Prim1	J04620	1.7
Mcm7	NM_008568	1.7
A4galt	BG064632	1.7
Hcn1	NM_010408	1.7
Macc1	BB007136	1.7
Dnajb4	BC017161	1.7
Maoa	AV356118	1.7
Mirhg1	AK017164	1.7
Pip5k1a	BB822856	1.7
OTTMUSG00000015563	AK013448	1.7
Vcan	BM251152	1.7
Sox4	AI428101	1.7
Nes	AK012622	1.7
Psap	BM212050	1.7
Prpf19	BC004070	1.7
Ccne2	AF091432	1.7
Galnt2	AF348968	1.7
Sema3d	BB499147	1.7
Cspg4	BB377873	1.7
BC020402	BB029175	1.7
Kitl	M64262	1.7
Vcan	NM_019389	1.7
Itga4	BB205589	1.7
Sesn2	AV308638	1.7
Enah	AV329519	1.7
Metrn	BE947704	1.7
Sdpr	AV064339	1.7
Pola1	NM_008892	1.7
OTTMUSG00000015563 /// Ppp1r14c	AK013448	1.7
Lasp1	BC010840	1.7
Dusp10	NM_022019	1.7
Fam110c	NM_027828	1.7
St3gal6	NM_018784	1.7

Elavl2	BB105998	1.7
Npnt	AA223007	1.7
Aff2	BB342212	1.7
Abcc1	NM_008576	1.7
Cspg4	BB377873	1.7
Serpinb1b	AF426025	1.7
Brd2	BI155271	1.7
Dtl	AV308327	1.7
Sema3a	NM_009152	1.7
Sprr1a	NM_009264	1.7
Rbmx	NM_011252	1.7
Nrn1	AK003046	1.7
Swap70	AK019882	1.7
4930402H24Rik	BQ173880	1.7
9130008F23Rik	BB763680	1.7
Utp6	BC025074	1.7
Kif22	BC003427	1.7
Cdc6	NM_011799	1.7
LOC627626	BB111245	1.7
D530037H12Rik	BG066910	1.7
C330027C09Rik	AU018569	1.7
Gjb2	AV239646	1.7
100040182 /// 677010 /// EG433003 /// EG619883 /// EG625281 /// EG664969 /// Rpl30	BB283415	1.7
Hspa1b	M12573	1.7
Gabra4	BB430205	1.7
Gja1	BB142324	1.7
Chtf18	BM233289	1.7
Cbx6	BC019942	1.7
Rab40c	AF422144	1.7
Kntc1	AW536884	1.7
2610002D18Rik	AK011279	1.7
2010300F17Rik	AK008491	1.7
2810055G20Rik	AK021336	1.6
D0H4S114	D45203	1.6
Sdc1	BI788645	1.6
Col10a1	NM_009925	1.6
Haus6	BB794620	1.6
Areg	NM_009704	1.6
Cd80	D16220	1.6
Sdpr	BE197945	1.6
Arl5a	BB811124	1.6
Rpl12	BG807990	1.6

Fam134c	BC016089	1.6
Zdhhc21	BI900142	1.6
Klf4	BG069413	1.6
Gja1	BB039269	1.6
Ddah1	BE283964	1.6
D0H4S114	BB369191	1.6
D2Ertd750e	AU019491	1.6
Nfib	BB092799	1.6
Psap	BM212050	1.6
Ung	BC004037	1.6
Melk	NM_010790	1.6
Col1a2	BB150460	1.6
Hspa1b	M12573	1.6
Fam65b	BM242294	1.6
Erf	BB453531	1.6
Slc7a11	BB453858	1.6
Dhfr	NM_010049	1.6
Pcdh18	BM218630	1.6
Aldh1a7	NM_011921	1.6
C77370	AW495307	1.6
Baz1b	BB253608	1.6
2810026P18Rik	AK012825	1.6
Tcf19	BC004617	1.6
Galnt2	BG064057	1.6
Ywhag	NM_018871	1.6
Uhrf1	BB702754	1.6
Tmem121	AF488729	1.6
Nrcam	BB202655	1.6
Nufip2	AV112972	1.6
Sh3kbp1	AK007283	1.6
Pappa	AF439513	1.6
Uhrf1	BB702754	1.6
Sec61a1	BC003707	1.6
Tcf20	AW552808	1.6
Mcm7	NM_008568	1.6
Prim1	J04620	1.6
Gja1	M63801	1.6
Mfap3l	AV280494	1.6
100042515 /// EG545555 /// EG546331 /// EG665056 /// ENSMUSG00000060128 /// Hmg1l1 /// Hmgb1 /// LOC100045972 /// LOC100046019 /// LOC637733	AV127023	1.6
Cck	NM_031161	1.6
Mtm1	BG976607	1.6

Foxp2	BM964154	1.6
Tmtc2	AK018506	1.6
Dpp8	BM939621	1.6
Mlf1ip	BB667813	1.6
Myh10	BQ176159	1.6
Fam131b	AW490145	1.6
D2Ertd750e	AK012148	1.6
Foxp2	AV322952	1.6
Kif11	BB827235	1.6
Ccna2	X75483	1.6
Gpr149	BB075339	1.6
Inhba	NM_008380	1.6
OTTMUSG00000015351	BB830168	1.6
Slc40a1	AF226613	1.6
Nes	AI413223	1.6
Zcchc5	BQ126004	1.6
Orc1l	BC015073	1.6
Ncam1	BB698413	1.6
Diras2	BM114282	1.6
Nmt2	AV167182	1.6
Sh3kbp1	AK018032	1.6
Hoxb7 /// Hoxb8	X13721	1.6
Dnm3os	BB542096	1.6
Rrm1	BB758819	1.6
Swap70	AV024531	1.6
Smc2	BI684556	1.6
Itga5	AW544851	1.6
Lmnb1	AA270173	1.6
Megf10	AK013855	1.6
Sgol1	BB410537	1.6
Flrt2	BB817332	1.6
Gorab	BB183144	1.6
Pcdh9	BB244656	1.6
Nmt2	AI503912	1.6
Npnt	AA223007	1.6
Kdm4a	AA415022	1.6
100039963 /// Sema3a	NM_009152	1.6
Hoxb9	AA386586	1.6
Kif22	BC003427	1.6
Flnb	BB667380	1.6
Casc5	BB818947	1.6
Pappa	BB635017	1.6
Kif2c	BB104669	1.6

Trib2	BB354684	1.6
Calhm2	NM_133746	1.6
Rpa1	BM244983	1.6
Lmo4	NM_010723	1.6
Anp32a	AF022957	1.6
Pdgfc	NM_019971	1.6
Cdt1	AF477481	1.6
C77370	C77386	1.6
Rai14	BB308974	1.6
Herc3	AK017531	1.6
Hspa4	BB541289	1.6
100040123 /// EG383032 /// EG665772 /// Rps17	AA030209	1.6
Ptprd	BB075247	1.6
Flrt2	AW555664	1.6
Gja1	AV330726	1.6
Serpinb1a	AF426024	1.6
Wdhd1	C77437	1.6
Mcm7	BB407228	1.6
Cd44	X66083	1.6
Dis3	BM232345	1.6
Ogn	BB542051	1.6
Hnrnpul2	BI080136	1.6
Usp1	BC018179	1.6
Rg9mtd2	AV214521	1.6
Stom	AF093620	1.6
Plk1	NM_011121	1.5
Asb5	NM_029569	1.5
Pnn	AV135835	1.5
Atad5	BB431627	1.5
Ccnd2	NM_009829	1.5
---	BB091802	1.5
Klf7	BB524597	1.5
Nudt21	BG070110	1.5
F630043A04Rik	BG073400	1.5
Foxp1	BG962849	1.5
Col6a3	AF064749	1.5
Mtm1	BG976607	1.5
Bub1b	AU045529	1.5
Aspm	NM_009791	1.5
Hmgb1	BF166000	1.5
Foxp1	BG962849	1.5
Tnfrsf11b	AB013898	1.5
Kif4	NM_008446	1.5

Unc5b	AK018177	1.5
Hipk2	AF208292	1.5
Anln	BI690018	1.5
Ppap2a	NM_008903	1.5
Ankrd28	AV261293	1.5
Zwilch	BC027435	1.5
Mki67	X82786	1.5
Mad2l1	NM_019499	1.5
LOC100048299 /// Max	AA617392	1.5
Dpysl3	AV161550	1.5
Uty	BB742957	1.5
Sec61a1	BC003707	1.5
Shcbp1	NM_011369	1.5
Egln3	BC022961	1.5
Fus	AF224264	1.5
Zfpm2	NM_011766	1.5
Rpa1	BB491281	1.5
Hoxa3	BB496114	1.5
Rad51ap1	BC003738	1.5
Ncapg	BB702347	1.5
Hmga2-ps1	AV377334	1.5
S1pr3	BB532532	1.5
Ivns1abp	NM_028582	1.5
Mtap4	BE197560	1.5
Itga6	BM935811	1.5
Zfp101	BC002058	1.5
Smc4	AV172948	1.5
Gins2	AW488914	1.5
Pcdh18	BM218630	1.5
LOC100270747	BB200448	1.5
Cct4	NM_009837	1.5
Mmp14	NM_008608	1.5
Racgap1	AF212320	1.5
Clspn	BG067086	1.5
Cdkn2c	BC027026	1.5
Matn2	BB338441	1.5
2810417H13Rik	AK017673	1.5
Usp1	BC018179	1.5
Rgs16	U72881	1.5
Foxs1	BB040642	1.5
Rbbp4	BF011461	1.5
LOC100047340 /// Rcc2	AV122997	1.5
St3gal6	NM_018784	1.5

Chaf1b	BC013532	1.5
Kcnk2	NM_010607	1.5
Cdca7	AK011289	1.5
Dnm3os	BB542096	1.5
6430598A04Rik	BB387298	1.5
Abca5	BM937648	1.5
Col5a2	AV229424	1.5
Ncapg	BB702347	1.5
Alcam	U95030	1.5
Tead2	D50563	1.5
Mfap3l	AK017269	1.5
A230058F20Rik	AV327739	1.5
Mcm7	BB464359	1.5
Kdm2a	BE690994	1.5
Cdca8	BB702047	1.5
Ccdc68	AV378320	1.5
LOC676546 /// Mmd	AA472735	1.5
B130021B11Rik	BM119919	1.5
Kif20b	BB200034	1.5
Malat1	AW012617	1.5
D13Ertd787e	AU020421	1.5
Ddit4	AK017926	1.5
Loxl3	NM_013586	1.5
Tacc3	NM_011524	1.5
Cct4	AV103196	1.5
Tk1	NM_009387	1.5
2700078E11Rik	BB137173	1.5
Pmm1	BI739353	1.5
Ar	AV232123	1.5
Hells	NM_008234	1.5
E2f8	BM247465	1.5
Pcdh9	BQ177394	1.5
Syncrip	BG920261	1.5
Rg9mtd2	BG063557	1.5
Tnik	AI117633	1.5
Calu	BB120190	1.5
Hnrnpr	BB822465	1.5
Arih2	NM_011790	1.5
Ccnb1	AU015121	1.5
Enah	BQ044016	1.5
Trim35	AB060155	1.5
Pif1	AV094878	1.5
Rrm1	BB758819	1.5

Sox4	AI428101	1.5
Sema3c	NM_013657	1.5
Klf6	AF072403	1.5
Asph	AF289490	1.5
Ahctf1	BM247201	1.5
Adam15	BC009132	1.5
Fscn1	NM_007984	1.5
Flrt2	BG075699	1.5
Rad54l	AV310220	1.5
Hspa1b	M12573	1.5
Cdca3	BI081061	1.5
Ptn	BC002064	1.5
Ttll12	BB481662	1.5
Dnajc7	NM_019795	1.5
Nr4a2	BB703394	1.5
Nuf2	AK010351	1.5
Sfrs5	AW212917	1.5
Sema6d	BB462688	1.5
Ogn	BB542051	1.5
Cdca8	AV307110	1.5
Fads2	NM_019699	1.5
Pdlim5	AK009464	1.5
Btg1	BE632903	1.5
Bbx	BF319769	1.5
Cdkn3	AK010426	1.5
Sf3b3	AK017529	1.5
Taf1d	AV167760	1.5
Pdlim5	NM_022554	1.5
Cdh3	X06340	1.5
Haus6	BB827546	1.5
Nrp1	AK011144	1.5
Ndc80	NM_023294	1.5
Khdrbs3	AK014353	1.5
Gins2	AW488914	1.5
Arl15	BB445175	1.5
Klf6	C86813	1.5
D16Ertd780e	BG069687	1.5
Rabgap1	BM223600	1.5
Mre11a	NM_018736	1.5
Ctdsp2 /// ENSMUSG00000040540	BB294133	1.5
Gja1	BB043407	1.5
Osr1	NM_011859	1.5
Rad51ap1	BC003738	1.5

Syncrip	BG920261	1.5
Ankrd28	BG066840	1.5
Chek1	BB298208	1.5
Sh3kbp1	BB766215	1.5
Aspm	BB648052	1.5
Trim59	AK012269	1.5
Nrp1	AK011144	1.5
Usp1	BC018179	1.5
Inppl1	BB769433	1.5
Ncam1	NM_010875	1.5
Pdgfc	NM_019971	1.5
Bat2	AK019427	1.5
Slc16a4	AV231970	1.5
Exo1	BE986864	1.5
Pbk	NM_023209	1.5
H2afy2 /// H2afy3	NM_026230	1.5
Dleu2	AA189481	1.5
Cyp51	NM_020010	1.5
Klf7	BB524597	1.5
Birc5	BC004702	1.5
1810032O08Rik	BM502805	1.5
Mfap3l	AV262974	1.5
Fusip1	NM_010178	1.5
B130021B11Rik	BB386167	1.5
Lman1	BE981934	1.5
Alcam	U95030	1.5
Plxdc2	AK017369	1.5
Ubtf	BB832806	1.5
Nfkbiz	BM240058	1.5
Smc2	NM_008017	1.5
Nrp1	AV291009	1.5
Bub1	AF002823	1.5
Metrnl	BC024445	1.5
Casp3	D86352	1.5
Kpna6	BC004833	1.5
Sfrs2	AK011528	1.5
Usp47	BG071065	1.5
Hmgb1	AI648759	1.5
Gemin5	BB824003	1.5
Socs2	NM_007706	1.5
BC055324	AV132065	1.5
Tmeff2	NM_019790	1.5
Srebf2	BM123132	1.5

Rnps1	NM_009070	1.5
Smc4	BI665568	1.5
Agap3	AF459091	1.5
Tulp4	BB667130	1.5
Suv39h2	NM_022724	1.5
Epb4.1l2	BE951907	1.5
Rtn4	BG072267	1.5
Aurkb	BC003261	1.5
Dpy19l1	BM119324	1.5
Lsm2	AF204156	1.5
Ppp3r1	NM_024459	1.5
EG383815 /// EG547267 /// EG668041 /// LOC677113 /// Rps24	BM119287	1.5
Klf7	BB524597	1.5
1110019D14Rik	AK003812	1.5
Vamp3	NM_009498	1.5
Plk4	AI385771	1.5
Sprr2h	NM_011474	1.5
Gyk	BF683028	1.5
Ssrp1	BC024835	1.5
Rgs2	AF215668	1.5
Klc1	AU079968	1.5
Sdpr	BE197945	1.5
Pde4b	BM246564	1.5
Wee1	NM_009516	1.5
9430008C03Rik	BF466702	1.5
AW551984	AV220682	1.5
Smoc2	AK006809	1.5
Ccna2	X75483	1.5
Hmga1	NM_016660	1.5
Prc1	BC005475	1.5
Upregulated genes		
Bex1	NM_009052	14.0
Krt18	NM_010664	11.9
Plcxd1	BB311508	9.1
Mpzl2	BC015076	7.3
Crym	NM_016669	7.2
Aard	AV256613	6.5
Mpzl2	BC015076	6.5
Cadm4	AY059394	6.4
Krt7	BC010337	6.2
Clu /// LOC100046120	AV152288	5.7
LOC100048346 /// Usp18	NM_011909	5.2

Ifi44	BB329808	5.2
Cdkn1c	NM_009876	4.8
Car3	NM_007606	4.7
Oasl2	BQ033138	4.6
Clu /// LOC100046120	AV075715	4.6
Bst1	AI647987	4.4
Afp	NM_007423	4.3
D630045M09Rik	BG069496	4.1
Trim30	AF220015	4.1
Prom1	NM_008935	4.0
Ifit1	NM_008331	3.9
Tgtp /// Tgtp2	NM_011579	3.9
Dsp	AV297961	3.8
Clu /// LOC100046120	NM_013492	3.7
Pla1a	NM_134102	3.6
Lyz1	AV066625	3.6
2010204K13Rik	NM_023450	3.6
Itih5	AK018605	3.6
Abhd3	NM_134130	3.6
H2-Q7	M29881	3.6
Nefl	M20480	3.5
Xaf1	BB645745	3.5
Apol9a /// Apol9b	BC020489	3.5
Synpo2l	BB322227	3.5
Dsp	AV297961	3.5
Iigp1	BM239828	3.5
Rtp4	BC024872	3.4
Cmpk2	AK004595	3.4
Angpt4	AV269710	3.3
AI451617 /// Trim30	BG068242	3.3
Iigp1	BM239828	3.3
Frmd4b	BB009122	3.3
677168 /// Isg15	AK019325	3.3
Trim63	BG817292	3.2
Spns2	BC025823	3.2
Lyz1	AV058500	3.2
Gbp3	NM_018734	3.2
Tnfsf9	NM_009404	3.2
Igtp	NM_018738	3.2
Trim30	BM240719	3.2
Slc2a3	BB414515	3.2
Clu /// LOC100046120	BB433678	3.1
Slc2a3	BB414515	3.1

Ifit3	NM_010501	3.1
Fxyd6	AB032010	3.1
C3	K02782	3.0
Loxl4	NM_053083	3.0
Irgm2	NM_019440	2.9
Aim1	BM233292	2.9
Il18	NM_008360	2.9
F5	NM_007976	2.9
Prr9	BB150166	2.9
Fgl2	BF136544	2.9
AI451617	BM241342	2.8
F5	NM_007976	2.8
Clip4	BM217861	2.8
Kng1	NM_023125	2.8
Rgs4	NM_009062	2.8
Hck	NM_010407	2.8
Fbxo2	BB311718	2.8
OTTMUSG00000025408	AU022548	2.7
Ms4a4d	NM_025658	2.7
Vnn1	AV360029	2.7
Afap1l2	BG068103	2.7
Phlda2	NM_009434	2.7
Lyz2	AW208566	2.7
Ifi203	BC008167	2.7
Wnt4	NM_009523	2.7
Cntf /// Zfp91 /// Zfp91-cntf	NM_053007	2.6
Cd38	BB256012	2.6
LOC671535 /// Plec1	BI525140	2.6
Mogat2	BB414982	2.6
Ccl8	NM_021443	2.6
Stat1	AW214029	2.6
Adssl1	NM_007421	2.6
Angpt4	NM_009641	2.6
Rsad2	BB741897	2.5
G530011O06Rik	BB276544	2.5
Vnn1	NM_011704	2.5
Wdr40b	BB274776	2.5
Sfrp1	BI658627	2.5
1190002H23Rik	BB408123	2.5
Acpp	BB008092	2.5
Gch1	BB698398	2.5
Liph	BB367422	2.5
Ifi205 /// Mnda	AI481797	2.5

Phyh	NM_010726	2.5
Plscr2	NM_008880	2.5
Cox7a1	AF037370	2.5
Ndrg1	AI987929	2.5
1700112E06Rik	BB246912	2.5
Ifih1	AY075132	2.4
Parp14	BC021340	2.4
Olr1	NM_138648	2.4
Gbp6	BM241271	2.4
Igfbp4	BC019836	2.4
Ecscr	BB736636	2.4
Mcpt8	NM_008572	2.4
Dock9	BB795072	2.4
Cadm1	NM_018770	2.4
Il6	NM_031168	2.4
Pstpip1	U87814	2.4
Ifi203	NM_008328	2.4
Lce3f /// LOC630971	AV076385	2.4
AI451557	AV277444	2.4
Rgs4	NM_009062	2.4
Cxcl14	AF252873	2.4
Gal3st1	AK002510	2.4
Ddx58	BB401061	2.4
Gbp2	BE197524	2.4
Tmem37	BC024613	2.4
Rsad2	BB132493	2.4
Slpi	NM_011414	2.4
Aldh1a2	NM_009022	2.4
Lcn2	X14607	2.4
H2-K1	BC011306	2.4
LOC100047963 /// Tor3a	AK009693	2.4
Cyb561	BC006732	2.4
Ndrg1	AV309418	2.4
1190002H23Rik	NM_025427	2.4
Akr1c21	AW146041	2.4
Mpa2l	BG092512	2.3
Rnf144b	AV274826	2.3
Pcdh21	NM_130878	2.3
Gbp2	NM_010260	2.3
H2-K1	S70184	2.3
Tmem86a	AK007864	2.3
Upk1b	BB427704	2.3
Stat2	AF088862	2.3

Steap4	NM_054098	2.3
H2-D1 /// H2-K1 /// LOC100044874	L23495	2.3
Igfbp3	AV175389	2.3
Abat	BF462185	2.3
Syt13	BB244585	2.3
Frmd4b	BG067753	2.3
Slc39a4	BC023498	2.3
BC006779	BE853170	2.3
Pfkfb3	NM_133232	2.3
Cd38	NM_007646	2.3
Krt80	NM_028770	2.3
Mocos	AK003797	2.3
Bace2	NM_019517	2.3
Icam1	BC008626	2.3
Smpdl3b	NM_133888	2.3
Oas1a	BC018470	2.3
Trim21	BC010580	2.2
Lgals3bp	NM_011150	2.2
Stat1	AW214029	2.2
Itga3	BI664675	2.2
Crispld2	BB745401	2.2
Dock9	BB795072	2.2
Dtx3l	BB705351	2.2
Apcdd1	BB271021	2.2
Tor3a	NM_023141	2.2
Isg20	BC022751	2.2
Dhx58	AF316999	2.2
677168	AK019325	2.2
Il11	NM_008350	2.2
Cxcl14	AF252873	2.2
Apcdd1	BB770932	2.2
Taf9b	AW555571	2.2
Bst2	BC008532	2.2
Adcy9	BB795229	2.2
Cxcl10	NM_021274	2.2
Sox7	NM_011446	2.2
Ablim1	BG065289	2.2
Ly6f	NM_008530	2.2
C1qtnf2	BF148029	2.2
Igfbp3	AI649005	2.2
Stard5	BI076697	2.2
Wdr40b	BB274776	2.2
2610019F03Rik	AK011462	2.2

Stat2	AF088862	2.2
Ntf5	AI462899	2.2
Psmb8	NM_010724	2.1
Exoc6	AV248277	2.1
Parp9	NM_030253	2.1
Susd2	AK004703	2.1
Gch1	NM_008102	2.1
2600010E01Rik	AK014682	2.1
Timp3	BI111620	2.1
Dtx3l	AV327407	2.1
Scel	NM_022886	2.1
Wnt7a	AK004683	2.1
Stat1	AW214029	2.1
Ehhadh	NM_023737	2.1
Fam174b	BG073439	2.1
Slc9a3r1	BB805362	2.1
Sord	AV253518	2.1
Csf1r	AI323359	2.1
Car2	NM_009801	2.1
Spon2	NM_133903	2.1
Mmp13	NM_008607	2.1
Timp3	BI111620	2.1
Sema3b	NM_009153	2.1
C920025E04Rik	NM_010398	2.1
Nkd2	BB767757	2.1
Sprr2a	NM_011468	2.1
D14Ertd668e	AV280841	2.1
Igfbp4	BB787243	2.1
Flt4	AI323512	2.1
Crispld2	BB558800	2.1
Aif1l	BC024599	2.1
Crispld2	AK019034	2.1
Abca1	BB144704	2.1
Mrgpre	BB373312	2.1
Prrg3	BB164509	2.1
Loxl4	NM_053083	2.1
Ptx3	NM_008987	2.1
Hp	NM_017370	2.0
Rab40b	AV364488	2.0
Ifi35	BC008158	2.0
Abcc3	AK006128	2.0
Afap1l1	BB106834	2.0
AI451617	BG068242	2.0

Axin2	BB398993	2.0
Ifi204	NM_008329	2.0
Sema4f	BB271145	2.0
Crabp2	BC018397	2.0
Maf	AV284857	2.0
Gzme	NM_010373	2.0
Cxcl1	BB554288	2.0
Reep6	AK002562	2.0
Nppb	NM_008726	2.0
Trim34	AF220142	2.0
Cxcl1	NM_008176	2.0
Sgcb	AI844814	2.0
Ifi35	AW986054	2.0
Rab3d	BB349707	2.0
4-Sep	NM_011129	2.0
Ifi35	AW986054	2.0
Timp3	BI111620	2.0
Selp	M72332	2.0
Spink2	BE456717	2.0
Dock9	AA410148	2.0
Tnfaip8	NM_134131	2.0
Galnt12	AV376137	2.0
2600010E01Rik	AK011178	2.0
Cda	AK008793	2.0
Als2cl	BM201174	2.0
Igfbp4	BB787243	2.0
9030409G11Rik	BQ175107	2.0
Irf9	NM_008394	2.0
Sncg	NM_011430	2.0
Nrip3	NM_020610	2.0
Tppp3	NM_026481	2.0
Gzme	NM_010373	2.0
Acsl6	BC022959	2.0
Ndrg1	NM_008681	2.0
AW987390	BB018051	1.9
100038993 /// Il11ra1 /// Il11ra2 /// OTTMUSG00000011351	BC004619	1.9
Rtn2	AF038538	1.9
Dync1i1	NM_010063	1.9
Eif4e3	BC027014	1.9
Irf7	NM_016850	1.9
Fndc3c1 /// LOC676436	BG065026	1.9
Pygl	NM_133198	1.9

Arvcf	BE947943	1.9
Card10	NM_130859	1.9
Glt8d2	AK003894	1.9
Ddx58	BG063981	1.9
Gpr123	AU015577	1.9
Sult4a1	AV338618	1.9
H2-M3	NM_013819	1.9
Hrh1 /// LOC100041871	BB051552	1.9
Cxcr6	NM_030712	1.9
Hs3st3b1	BG918344	1.9
Nap1l2	NM_008671	1.9
Lifr	AV246615	1.9
Nfkbie	BB820441	1.9
Tnip1	AJ242777	1.9
Aldh6a1	NM_134042	1.9
Cdkl2	NM_016912	1.9
Pmp22	NM_008885	1.9
Slco2a1	AI606070	1.9
Pdlim4	NM_019417	1.9
Esrp2	BF124648	1.9
Adcy7	NM_007406	1.9
Plat	NM_008872	1.9
Parp12	BM227980	1.9
Adam8	NM_007403	1.9
4930486L24Rik	AK015635	1.9
Galnt3	AK019995	1.9
Tspan9	AK020159	1.9
Bace2	BB558905	1.9
Herc5	AW208668	1.9
S100a13	NM_009113	1.9
Bat2d	BI083627	1.9
Cxcr6	AF301018	1.9
Tmem54	BC019563	1.9
Socs3	BB241535	1.9
Serpinb9g	AF425083	1.9
Slc9a3r1	BB805362	1.9
Selp	BB224329	1.9
Tmem51	BC003277	1.9
Trim54	NM_021447	1.9
Hint3	BM213104	1.9
Slco1a5	NM_130861	1.9
Igfbp4	BC019836	1.9
Arrb1	AK004614	1.9

Epb4.1l5	AW537770	1.9
Tcp11l2	BM245221	1.9
Xdh	AV286265	1.9
Cd274	NM_021893	1.9
B230311B06Rik	BB309504	1.9
Steap2	BB817972	1.9
Ildr2	BG067625	1.9
Radil	BB521978	1.9
C1r	NM_023143	1.9
Gbp6	BC010229	1.9
Arhgap18	BB667215	1.9
100040462 /// Ifi203 /// Ifi204 /// Ifi205 /// LOC192690 /// LOC640890 /// Mnda	AI481797	1.9
Igfbp4	NM_010517	1.9
Aqp1	NM_007472	1.9
Ivl	AV009441	1.8
Upk1b	BB219662	1.8
Mtss1	BC024131	1.8
Aldh1l1 /// LOC100047937	AK007822	1.8
Plcxd1	BB187908	1.8
Eif4e	BQ032226	1.8
Apcdd1	BB770932	1.8
Llgl2 /// LOC100047332	AY033650	1.8
Cand2	BM238658	1.8
Slco2a1	NM_033314	1.8
Boc	BB005556	1.8
Stard5	BI076697	1.8
Mmp3	NM_010809	1.8
Spint2	AV058358	1.8
Fuca2	BM054266	1.8
Pdcd6ip	BC026823	1.8
Cib2	NM_019686	1.8
Fhod3	BG066491	1.8
Igf2	NM_010514	1.8
Serpini1	NM_009250	1.8
Hpse	BG094050	1.8
Nmi	BC002019	1.8
Pfkfb4	BE136572	1.8
Ablim1	AK011936	1.8
Ptplad2	AV291250	1.8
Itih5	AV239969	1.8
Fam117a	AW548096	1.8
Slc7a7	NM_011405	1.8

Sfmbt2	BM200222	1.8
Krt20	AF473907	1.8
Yipf2	AV166218	1.8
Klc3	BC017147	1.8
Creg1	BC027426	1.8
Ttll7	BB795572	1.8
0610010O12Rik	AK002512	1.8
Pdlim2	BC024556	1.8
Prg4	NM_021400	1.8
Mbp	BB181247	1.8
AI256396	BB328287	1.8
Lhx6	AB031040	1.8
Ccl17	NM_011332	1.8
Mmp10	NM_019471	1.8
Phactr2	BE631955	1.8
Mest	AW555393	1.8
Scn3b	BE951842	1.8
Peg3	AB003040	1.8
Pla2g7	AK005158	1.8
Isyna1	NM_023627	1.8
Peg3	AB003040	1.8
S100a1	AI266795	1.8
Lynx1	NM_011838	1.8
Sfrp1	BI658627	1.8
Pdk1	BB553369	1.8
B4galt4	AF158746	1.8
1600014C10Rik	AV341544	1.8
Lrpap1	D00622	1.8
Tuft1	NM_011656	1.8
Hivep3	BB164127	1.8
Calml4	AY061807	1.8
9230105E10Rik	BI653857	1.8
Sord	BI143942	1.8
Gstm6	NM_008184	1.8
Svep1	NM_022814	1.8
Lynx1	BB431070	1.8
Rragd	BF462770	1.8
Ildr2	AI852300	1.8
Pla2g16	BC024581	1.8
Lor	NM_008508	1.8
Rgs4	NM_009062	1.8
Larp6	NM_026235	1.8
Ehd4	NM_133838	1.8

Rdh10	BG073496	1.8
Bace2	BB348062	1.8
Tm7sf2	BC014769	1.8
Gjb4	NM_008127	1.8
Ager	NM_007425	1.8
Pla2g16	BB404920	1.8
Smarca1	NM_053123	1.8
Chic1	BG065782	1.8
Socs3	BB831725	1.8
Optn	BB770843	1.7
Cxcl1	BB554288	1.7
2010012O05Rik	BB322051	1.7
0610037M15Rik	BG916808	1.7
Selp	M72332	1.7
Bnc1	U88064	1.7
Dgat2	AK002443	1.7
1190003J15Rik	BI556771	1.7
1110008P14Rik	C79326	1.7
4930583H14Rik	NM_026358	1.7
Dach2	NM_033605	1.7
P2rx5	NM_033321	1.7
Speg	NM_007463	1.7
Steap2	BB529332	1.7
Slc9a3r2	AV002797	1.7
LOC100045567 /// Pnp1 /// Pnp2	AK008143	1.7
Vamp5	AK009266	1.7
Rnasel	BF714880	1.7
Cyld	AK013508	1.7
Ccl20	AF099052	1.7
Samd9l	BB145092	1.7
Rom1	NM_009073	1.7
Akr1c18	NM_134066	1.7
Rasgrp3	BB042252	1.7
Sema3e	AF034744	1.7
LOC100045833 /// Ly6c1 /// Ly6c2	NM_010741	1.7
Acss2	NM_019811	1.7
Hdac11	BC016208	1.7
Sfrp1	AK008943	1.7
Smarca2	BM230202	1.7
Tbcel	BB540721	1.7
Nnat	AV218841	1.7
Abcb1a	M30697	1.7
Chmp4c	AK008733	1.7

Wnt4	AW047257	1.7
Cdon	AW557006	1.7
Cisd3	AV000569	1.7
Flywch2	BB251185	1.7
Car12	AK009873	1.7
Fam134b	BC019494	1.7
Rab3d	BB349707	1.7
Clip4	AK017914	1.7
Nipal2	BC016107	1.7
Cxadr	BE824924	1.7
Ube1l	AK004894	1.7
Pnkd	NM_019999	1.7
Mmp19	AF153199	1.7
Il13ra1	BI081033	1.7
Akr1c12 /// Akr1c13	AF177041	1.7
BC029722	AK009222	1.7
Wfs1	NM_011716	1.7
Entpd4 /// LOC100048085	BB022415	1.7
Rec8	NM_020002	1.7
Arhgap28	BB458819	1.7
Glt8d2	AK003894	1.7
Limch1	AV024662	1.7
Ckb	BG967663	1.7
Arhgef3	BC012262	1.7
Abcg1	AW413978	1.7
Npl	BC022734	1.7
Pde2a	BG069616	1.7
Atp8a1	AW610650	1.7
H2-Ke6	AI323545	1.7
Ctnnal1	BQ031240	1.7
C1qtnf5 /// Mfrp	BC023068	1.7
Rasgrp3	BB042252	1.7
Ppt1	AF326558	1.7
Nlrc3	BB466171	1.7
100039707 /// Mthfs	NM_026829	1.7
Glt8d4 /// LOC100048436	AV278332	1.7
Nkd2	BC019952	1.7
Nts	NM_024435	1.7
Fam49a	AV228737	1.7
Eif2ak2	AV328340	1.7
5730469M10Rik	AK017688	1.7
Acot11	AW060409	1.7
Tnfrsf22 /// Tnfrsf23	BB366863	1.7

Snhg11	BI731047	1.7
Lgals9	NM_010708	1.7
Nudt22	BC019768	1.7
Tbc1d24	AA270038	1.7
Sprr2a	AV371678	1.7
Ch25h	NM_009890	1.7
Hsd3b7	NM_133943	1.7
Pgf	NM_008827	1.7
Sh3bgrl2	BB352548	1.7
8430427H17Rik	AK018446	1.7
Ppbp	NM_023785	1.7
Afap1l2	BG068103	1.7
Fhit	AF055573	1.7
Ptges	BB730139	1.7
Tmem106a	AV024335	1.7
Znrf2	BG071922	1.7
Sft2d2	AV238378	1.7
LOC100045567 /// Pnp1	BC003788	1.7
Speer3	NM_027650	1.7
Ddc	AF071068	1.7
Scrn1	BF466917	1.7
Epas1	BI647951	1.7
100042616	BI133445	1.7
S100a3	AF087470	1.7
Pld1	BM228590	1.7
Fstl3	NM_031380	1.7
6-Sep	BG920446	1.6
Myo7a	NM_008663	1.6
Maff	BC022952	1.6
9530028C05	BQ175154	1.6
F630110N24Rik	AV307274	1.6
Tapbp	AF043943	1.6
Fam134b	NM_025459	1.6
Kifc3	NM_010631	1.6
H2-D1	M34962	1.6
H2-D1	M86502	1.6
Saa3	NM_011315	1.6
Tmem106a	BC022145	1.6
Calr3	AI324734	1.6
Tmem176a	BC006049	1.6
Ccl2	AF065933	1.6
Casp12	NM_009808	1.6
Upk1b	BB530943	1.6

Tmem8	NM_021793	1.6
Zbp1	AK008179	1.6
Rnf213	AW556558	1.6
Wnt9a	AV273409	1.6
Herc1	BM247513	1.6
Aifm2	AK017403	1.6
Mitf	BB763517	1.6
C77080	BB163333	1.6
Il13ra1	BB730912	1.6
Hdac5	NM_010412	1.6
Nebl	BM121794	1.6
Nmb	NM_026523	1.6
Gja3	BM125285	1.6
Has2	NM_008216	1.6
Ube2l6	BC008238	1.6
Rasgrp2	BE688720	1.6
Ninj1	NM_013610	1.6
Apoe	AK019319	1.6
Mvp	NM_080638	1.6
Plek2	NM_013738	1.6
Smpd3	BF456582	1.6
Casp4	NM_007609	1.6
LOC552880	BB028429	1.6
Reck	NM_016678	1.6
Nudt22	BC019768	1.6
Ccl9	AF128196	1.6
Trp53inp2	AK003956	1.6
Eif2ak2	BE911144	1.6
2310030G06Rik	NM_025865	1.6
Creg1	BC027426	1.6
Kif5c	BB698320	1.6
C1s /// LOC100044326	BC022123	1.6
Aoc3	NM_009675	1.6
Lgals3	X16834	1.6
Mtm1	NM_019926	1.6
8430427H17Rik	AK018446	1.6
Rnf207	BI734893	1.6
D330022A01Rik /// Ube1l	AK004894	1.6
Trf	AF440692	1.6
As3mt	AK009814	1.6
Rrm2b	BB702377	1.6
Ap3m2	BC027301	1.6
Sned1	BB487754	1.6

Cxcl16	BC019961	1.6
Cd99l2	BB334959	1.6
Optn	AK015354	1.6
H2-D1	L36068	1.6
Rassf7	NM_025886	1.6
Mfsd6	BF225441	1.6
Gstm2	NM_008183	1.6
Ninj1	AU024536	1.6
6330512M04Rik	BM116861	1.6
Serpinb8	BB049357	1.6
Steap2	BE995447	1.6
Tinagl1	BC005738	1.6
Mpp7	AK012883	1.6
C920025E04Rik /// H2-T23	NM_010398	1.6
Tbc1d24	BF536757	1.6
Speg	NM_007463	1.6
Sytl4	NM_013757	1.6
1110008P14Rik	BC024615	1.6
Htra3	NM_030127	1.6
Adamts4	BG064671	1.6
Sgcb	AK014381	1.6
Usp2	AI553394	1.6
Dmxl2	AK018275	1.6
4632428N05Rik	BC003967	1.6
Enpp4	BG920295	1.6
Olfml3	NM_133859	1.6
Ndrg1	AI987929	1.6
Hsdl2	BM200015	1.6
Mansc1	AK002644	1.6
Brp44l	AV223468	1.6
Cd99l2	BB038546	1.6
Hspa12a	BQ177161	1.6
H2-T10 /// H2-T17 /// H2-T22 /// H2-T9	NM_010395	1.6
Arvcf	BE947943	1.6
Naprt1	AI174034	1.6
LOC100034363 /// Tmsb15b1-Tmsb15b2	AW912417	1.6
Acaa1b	BC019882	1.6
Parp4	BB552308	1.6
Atp9a	AF011336	1.6
Shroom3	NM_015756	1.6
Stard10	NM_019990	1.6
Tnfsf11	NM_011613	1.6
Cnp	BB251922	1.6

Il13ra1	BB730912	1.6
Stard8	BM119481	1.6
Xkr8	AV273072	1.6
Cd40	NM_011611	1.6
Elovl4	BB829575	1.6
Acss2	NM_019811	1.6
Ndrg2	NM_013864	1.6
Stx11	BB767243	1.6
Ppp2r2c	AV223153	1.6
Sdsl	NM_133902	1.6
Ptprg	AK017277	1.6
Dusp2	L11330	1.6
Slc9a3r1	BG066200	1.6
Il13ra1	S80963	1.6
Serping1	NM_009776	1.6
Obfc2a	BE457727	1.6
Ppfia3	BG962793	1.6
Cxcl2	NM_009140	1.6
Zfp672	BC003258	1.6
Chst11	AK003880	1.6
Rbp1	NM_011254	1.6
Kcnmb1	BB633976	1.6
Tgfbi	BB532080	1.6
Dner	BB038556	1.6
Mgat4a	BB109391	1.6
Mfsd9	AU067683	1.6
Camk1	NM_133926	1.6
Morn4	BF464669	1.6
OTTMUSG00000016644	BM245961	1.6
Dlk1	NM_010052	1.6
Adcy9	AW125421	1.6
Kif21a	NM_016705	1.6
Nudt11	BQ174833	1.6
Taf7	AV213552	1.6
Ccpg1	BC006717	1.6
Fcgrt	NM_010189	1.6
Nol3	BC027290	1.6
Erap1	NM_030711	1.6
Shroom2	BQ176992	1.6
Cyld	BM119209	1.6
Dync2li1 /// LOC100048514	AK008822	1.6
Fam69b	NM_019833	1.6
H2-L	M69068	1.6

Ccl7	AF128193	1.6
Endod1	BF168366	1.6
Ifi27l2b	BC021795	1.6
Gpr116	AW547876	1.6
Pdzd2	AV376136	1.6
Golm1	BC011152	1.6
Aifm2	AK017403	1.6
Cpeb4	NM_026252	1.6
Cgnl1	BB409331	1.6
Casp12	NM_009808	1.6
5730469M10Rik	AV332575	1.6
Tgfbi	BB533460	1.6
Gm2a	BC004651	1.6
Sod3	NM_011435	1.6
Hfe	AJ306425	1.6
Aqp5 /// LOC100046616	NM_009701	1.6
Cyp27a1	NM_024264	1.6
A930005H10Rik	AV009179	1.6
Csf3	NM_009971	1.5
Herc3	BM239854	1.5
Tlr3	NM_126166	1.5
Mtap7	NM_008635	1.5
Tgfbi	NM_009369	1.5
Mkrn1	BC003329	1.5
Cd40	BB220422	1.5
Ostm1	AK004546	1.5
Cotl1	BB160417	1.5
Tmem154	BB778966	1.5
ENSMUSG00000073019	BB349472	1.5
Nudt14	BC025444	1.5
Slc2a13	BB191000	1.5
0610040B09Rik	AV302770	1.5
Napepld	BB325565	1.5
Ficd	C77487	1.5
Bicd1	BB130665	1.5
Bscl2	BB223872	1.5
BC023969	BI664409	1.5
Pion	BB820613	1.5
1810012P15Rik	AW108427	1.5
Ikbke	NM_019777	1.5
Scube3	BB484128	1.5
Tspan13	BB807707	1.5
Kif21a	BB342219	1.5

LOC545261	AI429562	1.5
Chmp2a	BC012230	1.5
Timp3	BI111620	1.5
Pcyox1	BB041555	1.5
Klhl29	BI988550	1.5
Phactr2	BB321846	1.5
6330416G13Rik	AV326978	1.5
Tmem141	AW551717	1.5
5133401N09Rik	BC026742	1.5
Nlrx1	BB830346	1.5
Pgcp	BB468025	1.5
Lrpap1	D00622	1.5
Commd9	AK007640	1.5
Insl6	NM_013754	1.5
Gpm6b	AK016567	1.5
St14	NM_011176	1.5
1810020D17Rik	BC026557	1.5
Arrdc4	BC025091	1.5
Fbxo6	NM_015797	1.5
Tst	BC005644	1.5
Ninj1	BB252065	1.5
Ank2	BQ174638	1.5
Sbsn	AI507307	1.5
Cd40	AI385482	1.5
Acat1	BG070487	1.5
Cyb561d2	NM_019720	1.5
Rab3d	BB349707	1.5
Plekha2	BE852755	1.5
Kif21b	AV122249	1.5
Vav3	BC027242	1.5
Aifm2	BB772185	1.5
Prkcz	NM_008860	1.5
Plekhh2	AW122265	1.5
Tmem38b	BC011072	1.5
Ctf1	NM_007795	1.5
Entpd5	NM_007647	1.5
Hagh	BC004749	1.5
Fam73a	BB375245	1.5
Rnaset2a /// Rnaset2b	BI410170	1.5
Prlr	AW554594	1.5
Lrpap1	AV309553	1.5
2610318N02Rik	AK012048	1.5
Adar	AF291876	1.5

Ppfibp2	NM_008905	1.5
Adcy7	BB746807	1.5
Sub1	BE989104	1.5
Nme3	NM_019730	1.5
S100a16	AV074236	1.5
Adamtsl1	AV380797	1.5
Sema3e	NM_011348	1.5
Bcl2l11	BM120925	1.5
Bscl2	AF069954	1.5
Adcy9	AW125421	1.5
Hagh	BC004749	1.5
Clybl	BC023398	1.5
U90926	NM_020562	1.5
Adar	BB308291	1.5
Dgat2	AK002443	1.5
Fars2	BB530332	1.5
Depdc6	AK014624	1.5
9030409G11Rik	AK018497	1.5
ENSMUSG00000071543	BB321858	1.5
Casc4	AV311104	1.5
Galnt10	BG965198	1.5
6530401D17Rik	BC016270	1.5
Ap1gbp1	C76297	1.5
Hspa12a	BB197697	1.5
Mitd1	BC020137	1.5
Slfn10	BB227643	1.5
Ifi203	M74124	1.5
Gpr123	BI135044	1.5
Sesn3	NM_030261	1.5
D16H22S680E	NM_138583	1.5
Gmpr /// LOC100045393	NM_025508	1.5
Ncoa7	BE686893	1.5
Slc2a9	BB148652	1.5
Clcn3	BI739053	1.5
---	BI150812	1.5
Endod1	BF168366	1.5
Igf1	BG075165	1.5
Cdk2ap2	NM_026373	1.5
Stx11	AK017897	1.5
A830007P12Rik	BC013092	1.5
Cpeb3	BB281000	1.5
Vdr	AV290079	1.5
1110003E01Rik	BB701294	1.5

Tln2	BQ174291	1.5
Psph	NM_133900	1.5
Bckdhb	AW047304	1.5
Mreg	AV298358	1.5
Ifi27l1	AW554405	1.5
A530017D24Rik	BQ174983	1.5
Ifitm1	BC027285	1.5
Nudt17	AK019109	1.5
Syt11	BF457392	1.5
Tmem38b	C77858	1.5
Kif5c	AI844677	1.5
Usp20	AK006800	1.5
Lipa	AI596237	1.5
Ids	BB493523	1.5
Aadacl1	AV369935	1.5
Enpp4	AV280361	1.5
Tnfrsf18	AF229434	1.5
Tmem173	AV300716	1.5
S100a1	BC005590	1.5
Fkbp11	NM_024169	1.5
Zfyve27	BB780581	1.5
Rab20	BG066967	1.5
Vgf	BF458396	1.5
Pdxk	BG063905	1.5
Fam122b	AK019480	1.5
Lipa	AI596237	1.5
2900026A02Rik	BG063749	1.5
Camk2n2	AK013788	1.5
Pcbd1	NM_025273	1.5
Mtss1	AV024771	1.5
Enpp5	BC011294	1.5
Rsph1	NM_025290	1.5
H6pd	BC027358	1.5
Wrn	D86527	1.5
Efna1	D38146	1.5
Rap1gap	AK005063	1.5
Entpd5	NM_007647	1.5
Akr1c13	NM_013778	1.5
Pilrb1	NM_133209	1.5
1190003J15Rik	AK013117	1.5
Ccdc23	BC002274	1.5
2010107G23Rik	BC024943	1.5
Dhrs11	BC022224	1.5

Prickle2	BQ177191	1.5
Mfsd8	AV024565	1.5
Lrpap1	D00622	1.5
2610110G12Rik	AK011838	1.5
Gpsm3	NM_134116	1.5
Cacng8	BQ266161	1.5
Tmem40	BB468188	1.5
Tgoln1	AI314055	1.5
Tmem42	NM_025339	1.5
Asah2	NM_018830	1.5
Madd	BM225074	1.5
Smpdl3a	NM_020561	1.5
9130213B05Rik	BC006604	1.5
Ccdc74a	BG068839	1.5
Ddb2	AY027937	1.5
Trpv2	NM_011706	1.5
Synpo	BB426294	1.5
Ereg	NM_007950	1.5
Slco2a1	NM_033314	1.5
Aadacl1	AV369935	1.5
Trim25	D63902	1.5
Gdap1	AU017649	1.5
Higd1a	NM_019814	1.5
Kidins220	BB430142	1.5
Actn3	NM_013456	1.5
Mpg	AV131794	1.5
Gcnt2	AB037596	1.5
Pcyox1	BB785407	1.5
Irak3	AV228493	1.5
Amot	BG067039	1.5
Maob	BB549292	1.5
H2-D1	M33151	1.5
Prss22	NM_133731	1.5
Pfkfb2	AV256368	1.5
Paqr7	BC022922	1.5
Slfn8	BC024709	1.5
Ahcyl2	BG072404	1.5
Ern1	BG075179	1.5
Dtd1 /// LOC100048650	AI451865	1.5
Pon3	NM_008897	1.5
Slc41a3	BC011108	1.5
Cdadc1	BE200391	1.5
Tmem141	AW551717	1.5

Aldh5a1	BQ175320	1.5
Klc4	NM_029091	1.5
Ubxn2b	NM_026534	1.5
1110031I02Rik	NM_025402	1.5
Fkbp1b	NM_016863	1.5
Il13ra2	BC003723	1.5
Mkrn1	BE133749	1.5
Shb	BI408715	1.5
Abca3	AK007703	1.5
Pdk4	NM_013743	1.5
Syt11	BC025207	1.5
Dclk1	AW105916	1.5
Usp11	AI117611	1.5
Cacna1a	AB066608	1.5
Mpp5	AW258373	1.5
Psmb10	NM_013640	1.5
Rab15	NM_134050	1.5
Sgcb	AK014381	1.5
Mpzl3	BM246392	1.5
Ldhb	AV219418	1.5
Prkar1b	BB274009	1.5
Itga3	NM_013565	1.5
Fst	NM_008046	1.5
Ube2z	BB032870	1.5
A230050P20Rik	BB085904	1.5
Rnaset2a /// Rnaset2b	AV101824	1.5
Sf3b5	AU043053	1.5
Ebpl	BC027422	1.5
Cotl1	AI327078	1.5
Rhbdf2	BB005249	1.5
Commd9	BB264843	1.5
Spata13	AV271736	1.5
Gpc4	BB530689	1.5
Nsf	BB400581	1.5
9530058B02Rik	NM_026633	1.5
A930005H10Rik	BF318375	1.5
Fam105a	BM224662	1.5
Psmf1	BC012260	1.5
Ppp1r3c	BQ176864	1.5
Gmds	AI747296	1.5
Vav3	BC027242	1.5
Xlr3a /// Xlr3b /// Xlr3c	NM_011726	1.5
Ralgps2	AK008856	1.5

LOC100047530	BI735554	1.5
Igfbp6	NM_008344	1.5
Fdx1	D43690	1.5
Chchd6	BC011331	1.5
Fads3	BM235658	1.5
Gdf10	L42114	1.5
Tdrd7	BC025099	1.5
Fam102a	BC023470	1.5
Nudt6	BB043522	1.5
Stap2	BC026642	1.5
D730040F13Rik	AF031164	1.5
4933428G20Rik	BE988299	1.5
Aldoc	BC008184	1.5
Mmp23	NM_011985	1.5
Mkrn1	BQ176661	1.5
Retsat	BB775176	1.5

Supplementary Table S2: Top Biological Functions affected in Ada3 cells as obtained from ingenuity pathway analysis

Name	p-value	# Molecules
Diseases and Disorders		
Cancer	7.02E-27 - 4.66E-04	445
Dermatological Diseases and Conditions	2.53E-18 - 3.89E-04	105
Genetic Disorder	2.53E-18 - 4.66E-04	330
Gastrointestinal Disease	5.58E-18 - 4.66E-04	211
Inflammatory Response	7.65E-18 - 4.41E-04	222
Molecular and Cellular Functions		
Cell Death	1.76E-21 - 4.02E-04	359
Cellular Growth and Proliferation	1.40E-16 - 4.66E-04	389
Cellular Movement	2.48E-16 - 4.41E-04	229
Cellular Assembly and Organization	3.71E-11 - 4.27E-04	188
Cellular Function and Maintenance	3.71E-11 - 4.13E-04	174
Physiological System Development and Function		
Tissue Development	9.91E-16 - 4.27E-04	330
Organismal Survival	1.34E-12 - 5.77E-05	211
Hematological System Development and Function	2.69E-12 - 4.66E-04	224
Immune Cell Trafficking	2.69E-12 - 4.41E-04	120
Cardiovascular System Development and Function	3.03E-12 - 2.93E-04	144

Supplementary Table S3: Primers used for Real Time-qPCR

Oligo Name	Sequence 5' to 3'
p27 F	CAGAATCATAAGCCCCTGGA
p27 R	GGGGAACCGTCTGAAACATT
Skp2 F	TCCGAGCTGATCGGGTGTGCT
Skp2 R	TCGGAAGCTGCACATGCGCA
c-myc F	TGACCTAACTCGAGGAGGAGCTGGAATC
c-myc R	AAGTTTGAGGCAGTTAAAATTATGGCTGAAGC
β-actin F	GCGGACTGTTACTGAGCTGCGT
β-actin R	TGCTGTCGCCTTCACCGTTCC
Fbxo5 F	GGCACAATGAGTTCGTGGAGGTGG
Fbxo5 R	AGTTCCAGGCAAAGGACCCACT
Cenpf F	GTGGCAGCAGATCACAAAAGGTCA
Cenpf R	TCCCCACAGGCAGGCTCCTT
Cdc6 F	TGCCCAAAGAGGAGCGGCCT
Cdc6 R	AGAGGGGAAGGAACTTGGCCCC
Kntc1 F	CCCCTCAACGGTGCCCAGTG
Kntc1 R	GGCGCATGCCCAGTGTACTTGT
Kif11 F	CCAGCAAGGAGACCAGTCAGGACA
Kif11 R	TGGAGGTGTGAAGCGGCAGT
Cyclin A2 F	GAGCTGGCCTGAGTCATTGGCA
Cyclin A2 R	TGTTGGGCATGTTGTGGCGCT
Smc2 F	GGTGGTCAGAGGTCTCTAGTGGCT
Smc2 R	TCTTCCCAGCTTGACTCTGCGT
Anillin F	TGCCTGGCACCGAAGATGGTG
Anillin R	TGCAGAGAGCCAGTTCTTGGTGA
Cdkn1c-F	ACTGCTGCGGCCAATGCGAA
Cdkn1c-R	TGGGCTGCTCTACGCAACCATCT
Foxg1-F	TTCTAACACGGTGTGGAGTGTC
Foxg1-F	TTGTCAGGTTTGAATGAAATGG
Cyclin E2 F	AGGAATCAGCCCTTGCATTATC
Cyclin E2 R	CCCAGCTTAAATCTGGCAGAG
Keratin 18 F	CAAGTCTGCCGAAATCAGGGAC
Keratin 18 R	TCCAAGTTGATGTTCTGGTTTT
Icam1 F	TGTCAGCCACTGCCTTGGTA
Icam1 R	CAGGATCTGGTCCGCTAGCT

Interleukin-6 F	CACAGAGGATACCACTCCCAACA
Interleukin-6 R	TCCACGATTTCCCAGAGAACA

SUPPLEMENTARY REFERENCES

1. Liu, P., Jenkins, N. A., and Copeland, N. G. (2003) *Genome Res* **13**, 476-484
2. Zhao, X., Malhotra, G. K., Lele, S. M., Lele, M. S., West, W. W., Eudy, J. D., Band, H., and Band, V. *Proc Natl Acad Sci U S A* **107**, 14146-14151

Mammalian Alteration/Deficiency in Activation 3 (*Ada3*) Is Essential for Embryonic Development and Cell Cycle Progression

Shakur Mohibi, Channabasavaiah Basavaraju Gurumurthy, Alo Nag, Jun Wang, Sameer Mirza, Yousaf Mian, Meghan Quinn, Bryan Katafiasz, James Eudy, Sanjit Pandey, Chittibabu Guda, Mayumi Naramura, Hamid Band and Vimla Band

J. Biol. Chem. 2012, 287:29442-29456.
doi: 10.1074/jbc.M112.378901 originally published online June 26, 2012
